

REGENERATION OF CATHODE MATERIALS FROM USED LI-ION BATTERIES VIA A DIRECT RECYCLING PROCESS

by

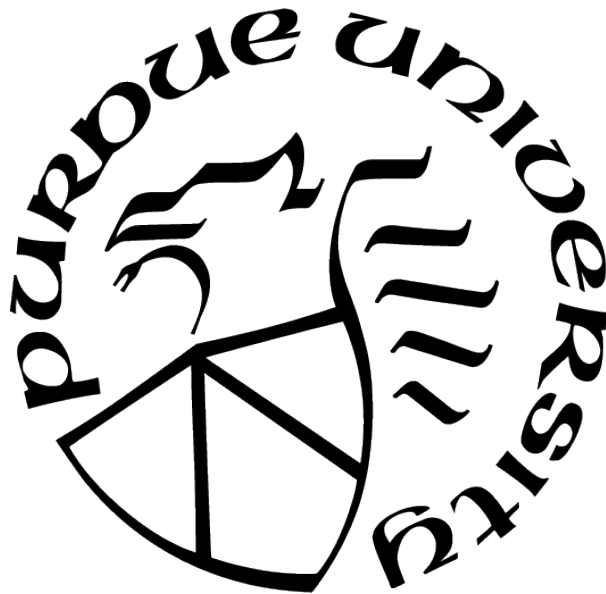
Hrishikesh Zurange

A Thesis

Submitted to the Faculty of Purdue University

In Partial Fulfillment of the Requirements for the degree of

Master of Science in Mechanical Engineering



Department of Mechanical and Energy Engineering

Indianapolis, Indiana

December 2020

**THE PURDUE UNIVERSITY GRADUATE SCHOOL
STATEMENT OF COMMITTEE APPROVAL**

Dr. Hosop Shin, Chair

Department of Mechanical and Energy Engineering

Dr. Likun Zhu

Department of Mechanical and Energy Engineering

Dr. Jing Zhang

Department of Mechanical and Energy Engineering

Approved by:

Dr. Likun Zhu

Dedicated to my loving family for their support
And to the scientists, activist and technologist working towards sustainable development
& green energy to fight climate change.

ACKNOWLEDGMENTS

Dr. Hosop Shin.- For helping me understand fundamentals of the field and teaching me required research & laboratory skills. He guided and supported me throughout the project.

Dr. Likun Zhu & Dr. Jing Zhang- For being on my committee and providing me helpful feedback. Also, for making the ET118 lab available to complete my research.

Nissan Motor Co.- For sponsoring our research project and providing us with battery materials and other resources.

Dr. Katerina Mazari & Dr. Miguel Cruz- Earth Science Department, IUPUI. For helping us to carry out ICP-OES study and their help in material digestion for sample preparation.

Department Of Mechanical & Energy Engineering, IUPUI- For providing support and resources and making the laboratories available for research work.

Michigan Technological University- For carrying out froth flotation experiment and providing us with the samples.

Colleagues & Friends- Dr. Yi & Dr. Li for helping in lab skills. Dr. Nojan A, Dr. Yadong Liu, Mr. PK Biswas, Mr. Daniel Minner, Mr. P. Nimbalkar for SEM and XRD trainings and discussions. Ms. A. Khadsare and Mr. M Jawalkar for computers and IT support.

TABLE OF CONTENTS

LIST OF FIGURES	7
ABSTRACT	9
1 INTRODUCTION	10
1.1 Motivation: Li-ion Battery Recycling	10
1.2 Literature Review	11
1.2.1 Technical aspect	11
1.2.2 Economic aspect	17
1.3 Backgrounds: Li-ion battery, cathode, and degradation.	19
1.3.1 Principles of Li-ion Batteries: Electrochemistry	19
1.3.2 Synthesis and characteristics of cathode materials	20
1.3.3 Degradation and aging mechanisms of LIBs	25
1.4 Objectives	30
2 EXPERIMENTAL METHODS	32
2.1 Materials	32
2.2 Recycling process: Cathode Liberation/Separation	32
2.2.1 Cell disassembly and electrode rinsing	32
2.2.2 Cathode material extraction	33
2.3 Recycling Process: Cathode Regeneration	34
2.4 Material Characterization: SEM/EDS, ICP, XRD, and TGA.	37
2.4.1 Scanning Electron Microscopy (SEM)	37
2.4.2 X-Ray Diffraction (XRD)	39
2.4.3 Inductively coupled plasma-optical emission spectroscopy (ICP-OES)	41
2.4.4 Thermogravimetric Analysis (TGA)	42
2.5 Battery Electrode Fabrication	44
2.5.1 Electrode Fabrication	44
2.5.2 Coin cell assembly	45

2.5.3	Coin cell Testing	46
3	RESULTS AND DISCUSSION	48
3.1	Separation effects (Ultrasonication vs. froth-flotation)	48
3.1.1	Morphology and purity: SEM/EDAX characterization	50
3.1.2	Chemical composition: ICP characterization	52
3.1.3	Electrochemical performance	53
3.2	Heat Treatment Effects	56
3.2.1	IPAD2 Cell: LCO case study	56
3.2.2	Nissan LEAF cell: LMO/LMC case study	58
3.3	Relithiation Process Effects	63
3.3.1	Molar ratio effect	63
3.3.2	Solvent effect (hydrothermal vs. solvothermal)	65
4	CONCLUSIONS AND FUTURE WORK	69
4.1	Conclusion	69
4.2	Future Work	70

LIST OF FIGURES

1.1	Charging/Discharging mechanism of LCO-based LIBs [16]	20
1.2	Working voltage and specific capacity of different cathode materials [26].	21
1.3	Different synthesis techniques utilized to produce cathode materials [26]	22
1.4	Layered structure of LCO [26].	23
1.5	Structural comparison between layered LiMnO ₂ structure and spinel LiMn ₂ O ₄ structure [29].	24
1.6	Cause and effect of degradation mechanisms and associated degradation modes of typical LIBs [37].	26
1.7	Schematic of the main causes of degradation in LIBs [37].	26
1.8	Battery capacity fade and possible internal mechanism in different stages [37].	27
2.1	The electrode rinsing procedure before cathode material extraction	33
2.2	The separation process using ultrasonication and centrifuge techniques	34
2.3	Hydrothermal reaction: a) hydrothermal reactor setup; (b) final product after synthesis.	35
2.4	A furnace used for heat-treatment process.	36
2.5	Schematic of SEM	38
2.6	An SEM image of a hydrothermally synthesized cathode material (Performed at IUPUI)	39
2.7	A Modern Automated X-ray Diffractometer	40
2.8	Working principle of an X-ray Diffractometer	40
2.9	ICP-OES instrument used for this study	41
2.10	Schematic of a typical thermogravimetric analyzer	43
2.11	A typical nature of the TGA curve	43
2.12	Coated cathode on aluminum foil (a) and a batch of coin cell cathodes punched out of it at IUPUI (b)	45
2.13	Architecture and assembly of a typical coin cell [56]	46
2.14	A CC-CV protocol between 3-4.2 V at a rate of C/10 used for initial cell cycle tests at IUPUI	47
2.15	‘ARBIN’ and ‘MTI 8-channel’ cell cycler setups used for cell testing in this research at IUPUI.	47

3.1	Liberation of cathode active material from aluminum foil as a result of ultrasonication	49
3.2	Different stages of removal of impurities using centrifuge: a) initial stage before centrifuge, b) after 1st centrifuge run, and c) 5 runs of the centrifuge	49
3.3	EDAX spectrum with the corresponding SEM image of cathode extracted from iPad2 cell using an ultrasonication-based separation technique	50
3.4	SEM images of cathode active material extracted by a) thermal treatment [58] and b) ultrasonication (our work)	51
3.5	Relative weight of constituent materials measured by ICP	52
3.6	The 1st and 2nd charge-discharge curves of cathodes recycled by ultrasonication separation from (a) Nissan LEAF cell (20% degraded) and (b) Apple iPad2 cell (minor degradation)	54
3.7	The charge and discharge curves for the 1st and 5th cycles of cells with cathodes separated from ultrasonication and froth flotation techniques	55
3.8	The 1st and 5th charge-discharge curves of heat-treated and non-heat-treated iPad cathodes	57
3.9	The 1st and 5th charge-discharge curves of heat-treated and non-heat-treated LEAF cathodes	58
3.10	Average discharged capacity observed at the 5th cycle in cells before and after heat treatment	59
3.11	The XRD patterns as observed for the reference unheated sample, 300 °C sample, 500 °C sample, and 700 °C sample	60
3.12	The 2nd charge-discharge curves of regenerated samples via hydrothermal synthesis with AM: LiOH ratios 1:1 and 1:5 and reference sample	64
3.13	SEM images of hydrothermally regenerated cathode powder (a, c) and reference cathode powder (b, d)	65
3.14	The 5th charge and discharge curves of reference, hydrothermal, and solvothermal samples and their capacity comparison	66
3.15	Relative weights percentage as determined by ICP for (a) LEAF reference powder and commercial NMC532 powder; (b) separated LEAF powder before and after hydrothermal regeneration	68

ABSTRACT

With the exponential rise in manufacturing and usage of Li-ion batteries (LIBs) in the last decade, a huge quantity of spent LIBs is getting scrapped every year. Along with the efforts to making more capable and safer batteries over the last three decades, there is an immediate need for recycling these scrapped batteries. Most of these batteries typically use lithium manganese oxide (LMO), lithium cobalt oxide (LCO), lithium iron phosphate (LFP), and lithium nickel manganese cobalt oxide (NMC) cathode chemistries, and developing a technique towards regenerating these cathodes can ensure huge economic and environmental benefits for the present and future. This research focuses on a set of direct regeneration techniques with the goal of regenerating used cathode materials to be reused in LIBs. Used Apple iPad2 batteries with LCO chemistry and Nissan LEAF batteries with a combination of LMO-NMC chemistry are selected for this research. The scope of research can be divided into two parts as liberation/separation of cathode material and regeneration of liberated cathode. The liberation/separation process is carried out with the aid of ultrasonication and organic solvents with the objective being keeping the morphology and chemical composition intact for a better quality of the material. The regeneration process uses a hydrothermal technique with variations of parameters. 1:1 and 1:5 molar ratios between cathode material and a lithium lithiation agent are chosen to understand the effects of the molar ratio on cathode regeneration. In addition, the effects of processing solution (water vs. a solvent) are examined by replacing water with TEG. The effects of heat treatment on cathode regeneration are also investigated by observing phase changes of materials at different temperatures.

1. INTRODUCTION

1.1 Motivation: Li-ion Battery Recycling

Lithium-ion batteries (LIBs) are the most prominent technological devices used for energy storage to achieve electromobility. The term ‘electromobility’ refers to an alternative transportation system based on vehicles propelled by electricity. Electromobility could solve problems related to both oil and biofuels whilst meeting our mobility needs and desires. With a tectonic shift happening in the automotive industry from conventional IC engines to battery-operated hybrid and electric vehicles (EVs), the number of batteries produced, consumed, and scrapped has been rising exponentially in recent years and is expected to follow a similar trend in the coming decade. The global electric vehicle market size was valued at \$118,864.5 million in 2017 and is projected to reach \$567,299.8 million by 2025, growing at a compound annual growth rate (CAGR) of 22.3% from 2018 to 2025 [1]. Simultaneously, it was also reported that the automobile industry itself will scrap 95 GWh worth of used LIBs by mid of the upcoming decade [2].

Taking into consideration the rapid growth of LIBs which leads to an increase in the number of dumped batteries at end of life every year, waste management of spent LIBs becomes significantly important. If the materials in dumped LIBs are not handled properly, it can cause major environmental issues in the near future due to the presence of hazardous battery components such as toxic electrolytes and flammable lithium-containing electrodes in LIBs.

From the economic point of view, decreasing the availability of the materials used in LIB cathodes, such as lithium (Li) and cobalt (Co), is another issue for the EV industry. Li and Co, which are widely used in LIBs, are scarce and mined in only a few countries, potentially creating risk in their supply and availability. For example, it is reported that, excluding the US, worldwide lithium production in 2019 decreased by 19% in 2018, which has made lithium supply security a top priority for many industries in the United States and Asia [3]. Recycling of LIBs can potentially be economically beneficial because it can reduce the cost of raw materials and help to ensure certain raw material supplies [4].

LIB recycling is key to securing the raw material supply for LIBs, while simultaneously protecting the environment. If a profitable LIB recycling technology is successfully developed, spent LIBs can be a viable secondary source for battery raw materials and they can be managed effectively, protecting the environment.

1.2 Literature Review

1.2.1 Technical aspect

Significant research has been done to establish optimal methods for recycling used LIBs. This section reviews the methodology and technical aspects of the recycling process. LiB recycling starts by extracting end-of-life (EOL) batteries from the EVs. Following the extraction, the batteries are disassembled down to module/cell level [5] and should be deactivated for safety reasons. The deactivation can be carried out by discharge of the whole battery systems, battery modules, and cells. Once the individual battery cells are deactivated, two distinct LIB recycling approaches, namely the indirect approach and direct approach, are currently employed. Both approaches follow different objectives and methodologies.

The indirect approach is to recover individual chemical elements, such as Li, Co, Ni, Cu, and Al, from spent LIBs. The recovered constituent materials can be used for other applications or they can potentially be reused for making new battery materials with additional manufacturing processes. The indirect approach is typically achieved by mechanical treatment followed by a pyrometallurgical or hydrometallurgical process. Mechanical treatment consists of crushing, classification, and sorting processes, in which highly valuable battery materials, including electrode materials, are extracted, and sorted for the next step, pyrometallurgical and/or hydrometallurgical process.

The pyrometallurgical process is a recycling technique aiming at recovering valuable metal elements from the LIBs in the form of metals or alloys. In this process, spent LIBs are fed into a furnace and smelted at high temperature ($>1000^{\circ}\text{C}$) decomposing plastics, electrolyte, and carbonaceous components. High temperatures, in the range of $500\text{-}600^{\circ}\text{C}$ are reported to be optimal to decompose polyvinylidene fluoride (PVDF) binder mostly used in commercial LIBs, resulting in separating active electrode materials from current collectors.

As a result of binder decomposition, the battery components are separated and metals such as Li, Al, Fe get concentrated in the slug, while metals (such as Co, Ni, and Cu) form alloys. If needed, the metals forming the alloys can be further separated into constituent metals using methods such as hydrometallurgy [6, 7]. Being a simpler method and effective for large scale operations, pyrometallurgy is widely used in battery recycling. However, there are certain drawbacks, including less effectiveness for recycling Li and complete failure to recycle separator, graphite anode, and other carbon-containing components. In addition, the process of burning demands high energy and causes the emission of hazardous gases to the atmosphere which reduced its environmental benefits significantly [8].

The hydrometallurgical process involves acids to leach valuable metals into solutions, recovering Co, Ni, Mn, and Li, from the mechanically separated battery materials. This process consists of two distinct steps, leaching/separation of metal ions followed by cathode regeneration from the formed leachate [8]. The key step in the hydrometallurgical process is the leaching of the various valuable metals from the cathode into a solution state. Depending on the different leaching agents, leaching can be categorized into inorganic acid leaching, organic acid leaching, ammonia leaching, and bioleaching. There are certain aspects to take into consideration such as leaching rates (i.e., the reaction speed of the leaching process), leaching efficiency (i.e., the ratio of the number of ions in the leachate to the total amount of that material/species in the original cathode), environmental impact, economic benefits, and reliability for re-utilization [9]. The specific steps involved in this method depend on the desired outcome. For example, if extracting pure metal elements is the target, inorganic acid or organic acid leaching process is carried out, followed by precipitation of the leachate and solvent extraction, resulting in individual metal products. On the other hand, if cathode regeneration is the target, methods such as ammonia leaching, bioleaching, and mechanochemical methods can be utilized [8]. In addition, co-precipitation and sol-gel methods have been applied for regeneration purposes [8, 10]. Compared with other processes, the hydrometallurgical process is effective in terms of its high recovery efficiency, low impurity of content, and lower usage of energy. Owing to these factors, hydrometallurgy is mainly used for the extraction of metals from used LIBs in indirect recycling approaches [8].

The major drawbacks of the indirect recycling approach are changes in material structure and secondary quality of extracted materials. Due to the extensive processes employed, materials often undergo undesirable structural changes that affect their reusability in batteries negatively. In addition, even if the materials are extracted for other applications, they are considered of lower quality compared to pristine materials which significantly reduces the economic benefits of recycling. Another important challenge is associated with the mechanical treatment in which the separation of current collector foils and electrochemical active coating materials is difficult to achieve [11].

Aware of the challenges above, recent LIB recycling research is directed toward recovering valuable battery components directly in reusable forms, retaining the original functional forms. This approach is called direct LIB recycling. This direct approach aims to minimize the destruction of the original structure of battery materials and regain the electrochemical performance of used battery materials. This approach could potentially achieve higher efficiency and lower environmental impact along with comparatively higher economic incentives. It enables the recovery of cathode materials in forms closer to be directly used in new cell production and thus the energy of the production can be significantly reduced [12].

The direct approach focuses on recovering valuable cathode materials from spent LIBs and involves two major steps: physical liberation/separation and regeneration. In the physical liberation/separation step, different components of the black mass (electrode material from the shredding of cells) are separated by physical processes, such as gravity separation, without causing chemical changes of the separated materials [12]. The separated cathode active materials are further inspected, and an effort is made to eliminate possible impurities caused by long-term cycling and the presence of liquid electrolytes. Once these impurities are eliminated, cathode active materials undergo the second step, the regeneration process, where the lost capacity is regained by reintroducing a certain amount of lithium into the cathode side to make up for the degradation over long term cycling. The regeneration process is carried out using several methods including hydrothermal synthesis and solid-state synthesis. In the process, the lost Li ions in the degraded cathode material are replenished through a relithiation process and further decomposition of residual PVDF binder is performed using heat-treatment, which is beneficial in terms of avoiding the particle agglomeration and en-

hancing the electrochemical performance of the obtained material. Moreover, the impurities on the spent materials are removed and the deteriorated structures, like the spinel and rock salt phases in LiNixCoyMnzO_2 , are converted back to the desirable layered structure [6]. The direct approach takes into consideration the fact that an EV battery is considered as the EOL stage after its original capacity fades to 80%. This indicates that the battery still possesses a significant energy storing capacity.

Various techniques have been applied to develop a direct LIB recycling approach so far. For the separation/liberation process, solvent dissolution, mechanical, and leaching methods have commonly employed, and their technical details are described below.

Solvent dissolution– The binders used in LIBs are generally PVDF or PTFE which are soluble in organic solvents. The presence of binders creates challenges in the separation of black mass from aluminum foil. Dissolving the binder material leads to an easier separation process. Dissolution also has additional benefits such as a low requirement of energy and its ability to preserve the crystalline structure of the active material, making it a preferred technique used in direct recycling [6]. Various organic solvents are used for this solvent dissolution process such as NMP, acetone, DMAC, DMF, etc. NMP and DMAC have been reported to be the most efficient and cost-effective for PVDF binders [10].

After the dissolution, a set of other processes is done to separate the black mass from the solution. Ultrasonication is commonly utilized at the beginning to aid the dissolution process by ensuring that the complete mass is separated from aluminum sheets. Additionally, centrifuge processes can be used to eliminate impurities from active materials. Followed by centrifuge, heating the wet material at temperatures around 100 °C helps to remove the organic solvents which yield pure black mass to be used directly for the regeneration process [13].

Separation using organic solvent dissolution is considered effective due to its ability to maintain the material structure and low energy requirements, however, the organic solvents tend to be too expensive and due to their toxicity, they are considered environmentally harmful [6].

Mechanical process– Certain mechanical processes are also being used for separation purposes recently [14]. Froth flotation is one of such established and widely used processes

for mineral processing, which can also be used for material separation. The nature of particles can be either hydrophilic or hydrophobic. Froth flotation uses these characteristics of materials to separate them from each other. With bubbles produced by a mechanical arrangement, the materials are extracted. A frother is used to carry hydrophobic materials to the surface as these materials tend to adhere to the formed bubbles. In contrast, the hydrophilic materials tend to sink, providing complete separation of materials in the process. The froth produced is collected and dried under vacuum to get separated products. This method is comparatively simpler and fast to perform. However, there can be certain problems associated with it. The main issue is that few materials in LIBs can get damaged due to water used over time, which can make it useless for regeneration [14].

Alkaline leaching– Given that Al is soluble in alkaline solution, alkaline leaching is a commonly used separating process with other methods like organic solvent dissolution. NaOH is a typically used solution to dissolve aluminum to separate cathode black mass in this process [14]. Additionally, the NaOH solution can also avoid the hydrolysis of LiPF₆, which generates poisonous HF gas, giving it a significant environmental benefit. However, as this method only causes dissolution of aluminum, the binders used in battery making such as PVDF are still present with the black mass which can be removed using the calcination process [14].

The separation/liberation process is followed by the regeneration of the separated cathode material. For the regeneration process, methods such as direct heat treatment, solid-state synthesis, hydrothermal synthesis, and solvothermal synthesis have been utilized in the literature and technical details are discussed below.

Direct heat treatment– This method has been mainly employed to regenerate LiFePO₄ batteries [15]. The PVDF binder present in the extracted cathode black mass causes agglomeration and results in the low tap densities of the untreated spent cathode particles which decrease the overall electrochemical performance. The material can be heated to temperatures of around 650 °C at which PVDF decomposes to ensure the elimination of binder materials. In addition, a study reported that new LiFePO₄ was formed from the FePO₄, Fe₂O₃, P₂O₅, and Li₃PO₄ that were derived from the decomposed LiFePO₄ materials during battery cycling [15]. The recovered cathode material showed a similar discharge capacity

as the pristine one. Hence, if the results are repetitive, this method can be used at the industrial level [15]. However, this process cannot solve the problem of Li deficiency in the degraded cathode.

Solid-state synthesis – In this method, the materials obtained from disassembled battery cathode are mixed with a certain chemical entity depending upon the chemistry and heat-treated to regain some of the lost lithium. The temperature ranges between 400 to 900 °C are typically used depending on the composition of cathode material and the high lithium entity used [15]. Different heating rates, variation in temperature, and a molar ratio of the mixing components affect end products, and hence they are needed to be controlled precisely. An optimal value for these conditions can be found experimentally for specific cathode materials and their SOC to yield better results. However, there are certain shortcomings associated with this method. The main issue is its inability to remove impurities in cathode materials like undesired MO₂, MO₃-type metal oxides formation at certain temperatures in the case of LMO rich cathode materials [10]. In addition, as solid-state synthesis uses mechanical processes during many steps, it can lead to issues like uneven mixing of raw materials which further leads to compromises in the properties of the product [10].

Hydrothermal synthesis– This method is one of the promising methods which can be implemented for direct regeneration of materials like LCO and LMO which are largely used in current battery production. This technique employs a close enclaved reactor to generate pressure and low temperature (100-200 °C) conditions in the presence of lithium salts for regeneration [15]. In this method, the cathode material extracted from used batteries is mixed in a solution containing lithium in abundance and the mixture is placed inside a reactor. The reactor is sealed to generate pressure. The system is further heated at temperatures higher than the solvent used in a lithium-containing solution. As the name indicates, water is often used as a solvent and hence the temperatures used are in the range of 120-200 °C, which is very low compared to those involved in solid-state synthesis methods [10]. The Li salts used vary with purpose and cathode materials; however, LiOH is most widely used as it is highly soluble in water to form a solution and can be used to regenerate various cathode materials e.g. LCO, LMO, and NMC. The amount of salt added for the process is determined based on the molar ratio and difference in molar ratios of the salt used. Based on a previous study,

it is known that molar ratio has the most impact on the regeneration compared to other factors like reaction time, temperature, and pressure [16]. All these conditions should be monitored precisely to determine the best possible combination for specific cathode materials. In the case of LCO, a study indicated that a molar ratio of 1:1 shows the best results [16]. The temperature conditions for this case ranged from 120 to 180 °C and the reported reaction time was from 14 hours to 22 hours. This method has considerable benefits over solid-state methods [16]. Reactions time can be shorter once the case-specific optimal combination is found. In addition, due to lower temperature reactions, the energy consumption is significantly less which is a significant cost saving parameter in industry scale operations. Most importantly, particles regenerated using the hydrothermal process tend to retain their original morphology and structure hence yielding better electrochemical performance as a result [15].

1.2.2 Economic aspect

Recycling of LIBs, especially with a direct recycling approach, has a significant value in terms of the economy. Researchers have developed various models to estimate recycling revenue, recycling cost and compared with the battery production cost [17]. Based on the EverBatt model, 8.17% of the cost can be saved by replacing the virgin materials with recycling components, where the cost of virgin production is about \$22.68 kg⁻¹ and that for spent LIB recovering is about \$20.81 kg⁻¹ [17]. The recycling process accounts for 25.91% of the total cost whereas cathode recycling comprises 17.41%. The cost of recycling and cathode manufacturing adds up to \$9.02 kg⁻¹. In this way, the calculated cost of cathode production can be saved up to \$1.29 kg⁻¹. The reduced cost represents the benefit of recovering the Co, Ni, Mn materials, accounting for 68.86% of the total cost savings [17]. In the EverBatt model of Argonne National Laboratory, recovered Co/Li/Mn/Ni compounds from cathode material were considered “good as new” by cathode powder producers and are therefore assumed to sell as their virgin counterparts, which means recycled batteries can help cut down costs for battery manufacturers and can also yield hefty economic benefits for the recycling industry [18].

The cost of raw materials plays a substantial role in the total costs, accounting for 64.28%. Besides, 6.43% of the total cost are attributable to the utilities. Among the material expenses, buying the spent batteries represents 87.05% of the overall expenditure due to the high price of the valuable metals in these batteries. It is estimated that recycling would be economically beneficial until the purchase price of spent LIBs reaches \$2.87 kg⁻¹ [17].

Another important advantage of recycling deals with the disposal cost of spent LIBs. Typical disposal costs fall in \$4,000-\$5,000 per ton. This includes shipping to the site and processing within a hazardous waste landfill. Since it is classified as a hazardous waste, the cost of safe disposal would be avoided by recycling [19].

Globally, the industry’s over-dependence on China has been showcased recently with the Coronavirus outbreak leading to disruptions in the supply of components. China, a battery manufacturing powerhouse is dealing with a slow down with the COVID-19 outbreak. The Chinese EV manufacturer BYD’s share has devalued by 10% since January 2020 [20]. Moreover, Jaguar Land Rover has paused the production of its I-pace electric SUV as is Mercedes of its EQC due to the unavailability of key gradients for batteries – including lithium and cobalt [21]. Battery recycling would be economically beneficial for automotive manufacturers to minimize the dependence on foreign sources of battery components. In January 2020, for example, the U.S. Department of Energy announced the creation of DOE’s first LIB recycling R&D Center, the ReCell Center [22].

Large fluctuations in the prices of raw battery materials cast uncertainty on the economy of recycling. The recent drop in cobalt’s price raises questions about whether the recycling of LIBs is a good business choice compared with manufacturing them with fresh raw materials. The recycled cobalt would struggle to compete with mined cobalt in terms of prices. Another long-term financial concern for LIB recycling companies is whether a different type of battery, such as Li-air, or a different propulsion system, like hydrogen-powered fuel cells, will gain a major foothold in the EV market in coming years, lowering the demand for LIB recycling [22].

In addition to material savings, LIB recycling has positive impacts on energy consumption and environmental protection. Li, Co, Ni, and Al production requires high energy to be extracted from the virgin resources and causes the emission of green-house gases (CHG)

from transportation and smelting processes. Recycling of other minor elements in LIBs such as Al, Cu, and Fe can save 95%, 85%, and 74% of the total energy required to obtain them through one extraction, respectively. Besides, most LIBs are currently disposed of in landfills unless restricted by municipal policies. Environmental hazards occur when water enters the landfill and leaches the toxic metals from LIBs. The issue is exacerbated by the fact that microorganisms in the landfills produce acids that can corrode the battery casing over time [23].

Various scientists have used life cycle analysis (LCA) to measure the environmental impacts of LIB recycling. Life-cycle environmental impacts of each recycling processes (pyrometallurgy, hydrometallurgy, etc.) is generally measured by considering three major categories: global warming potential over 100 years (GWP 100), expressed in kilograms of carbon dioxide equivalent (kg CO₂-eq), terrestrial ecotoxicity (TETP), and human toxicity potential (HTP). Both TETP and HTP are expressed in kilograms of dichlorobenzene equivalent (kg DCB-eq) [24]. With the assumption that the first large batch of EOL EVs would be treated around 2025, scientists estimated the recycling impact on energy consumption and greenhouse gas (GHG) emission in 2017. According to the study [25], although LIBs share only 9% of the whole EV by weight, it is estimated that 4.1 GJ and 1.2 tons CO₂-equivalent reduction in energy consumption and GHG emission by their recycling, accounting for about 13% and 23% reduction when entire EV is recycled.

1.3 Backgrounds: Li-ion battery, cathode, and degradation.

1.3.1 Principles of Li-ion Batteries: Electrochemistry

A battery is an energy storage device converting stored chemical energy to electrical energy and can be made of one or more electrochemical cells. Batteries can be divided as primary and secondary. In primary batteries, the chemical reaction is irreversible hence once discharged, they cannot be recharged and need to be scrapped. On the contrary, electrochemical reaction in secondary batteries is reversible allowing them to go through multiple charge-discharge cycles. The most widely used secondary batteries are LIBs. In LIB system, energy is stored when the battery is charged chemically through red-ox reactions

which used lithium intercalation between cathode and anode electrodes. The charging and discharging of battery are simply the back and forth movement of lithium ions between the two electrodes. The reaction in lithium ion batteries is reversible for thousands of cycles which makes LIBs usable for electromobility and portable devices.

An electrochemical cell is a system of a positive and a negative electrode separated by a porous separator between them in the presence of an ionic conducting electrolyte which works as the medium for ion transfer on both sides of the separator. Figure 1.1 illustrates the working mechanism of LIBs.

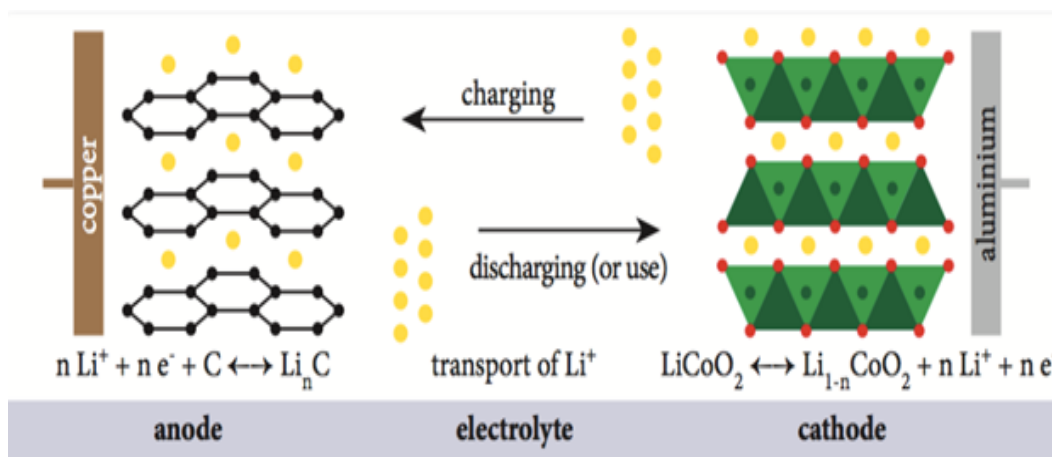


Figure 1.1. Charging/Discharging mechanism of LCO-based LIBs [16]

The anode is made of carbon/ graphite providing a high surface area and is usually plated on a copper current collector. The cathode is generally made using a lithium transition metal oxide like manganese, cobalt, nickel, etc. plated on an aluminum current collector. When the battery is being used, Li ions are transferred from the anode (oxidation occurs due to loss of electrons) through the intermediate electrolyte towards the cathode (reduction occurs due to gain of electrons).

1.3.2 Synthesis and characteristics of cathode materials

LiCoO₂ has been the dominant and first-generation cathode materials in commercialized LIBs throughout the initial battery development. Nowadays, many other cathode materials are being used in LIBs, which include layered LiNiO₂ and LiMnO₂ along with their

derivatives such as $\text{LiNi}_x\text{Co}_y\text{O}_2$, $\text{LiCo}_x\text{Ni}_y\text{Mn}_{1-x-y}\text{O}_2$, spinel-structured LiMn_2O_4 along with further derivatives such as $\text{LiNi}_x\text{Mn}_{2-x}\text{O}_4$ and $\text{LiCr}_x\text{Mn}_{2-x}\text{O}_4$, and olivine-structured LiFePO_4 . Cathode materials can primarily be categorized based on structure types. LiCoO_2 , LiNiO_2 , Li_2MnO_3 , $\text{LiNi}_{1-x}\text{Co}_x\text{O}_2$, $\text{LiNi}_{1/3}\text{Mn}_{1/3}\text{Co}_{1/3}\text{O}_2$, etc. have layered structures, while LiFePO_4 based materials have the olivine structure and LiMn_2O_4 is a spinel structure showing a three-dimensional framework [26, 27]. Cathode materials are selected based on the application to which the battery will be subjected to and the ability of the material to fulfill it. Factors such as operating voltage range, specific energy are vital for selection. Figure 1.2 shows a comparison between these factors for various cathode chemistries used. There exist a wide range of approaches for the synthesis of cathode materials. Although the processing parameters of these approaches vary with the chemistry used, some techniques are commonly used for different chemistries. Figure 1.3 represents the most widely used cathode synthesis techniques. The specific approaches used for cathode chemistry are described in subsequent sections.

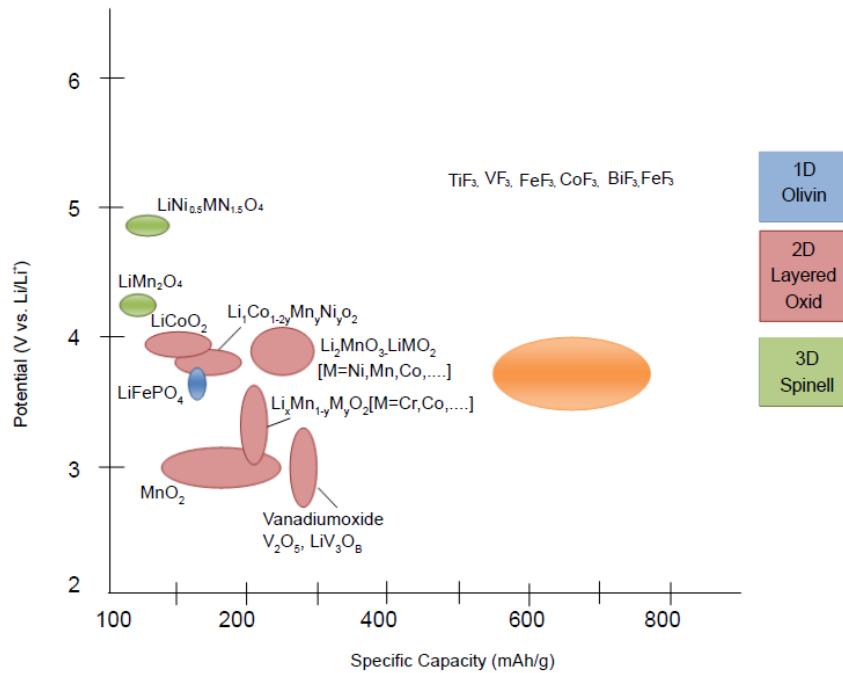


Figure 1.2. Working voltage and specific capacity of different cathode materials [26].



Figure 1.3. Different synthesis techniques utilized to produce cathode materials [26]

LCO (LiCoO_2)– This material was first reported by John B. Goodenough recognizing it has a layered structure and that lithium can be removed electrochemically, making it a promising cathode material. A LIB consisted of LCO cathode and carbon anode was first introduced commercially by Sony in 1991 [28]. LCO has -NaFeO_2 structure with O atoms present in a cubic closely packed FCC structure, when lithium is completely removed; the oxygen layers rearrange themselves to give hexagonal close packing in form of CoO_2 . Figure 1.4 represents the layered structure LCO [26].

The method of preparation of LCO includes solid-state reaction, sol-gel technique, ultrasonic spray pyrolysis, molten salt synthesis, co-precipitation method, freeze-drying method, complex formation method, hydrothermal synthesis, mechanochemical, and microwave synthesis, and other methods. Depending on the synthesis method, LCO could have either hexagonal layered for high-temperature LCO or cubic spinel-like structure for low-temperature LCO [26].

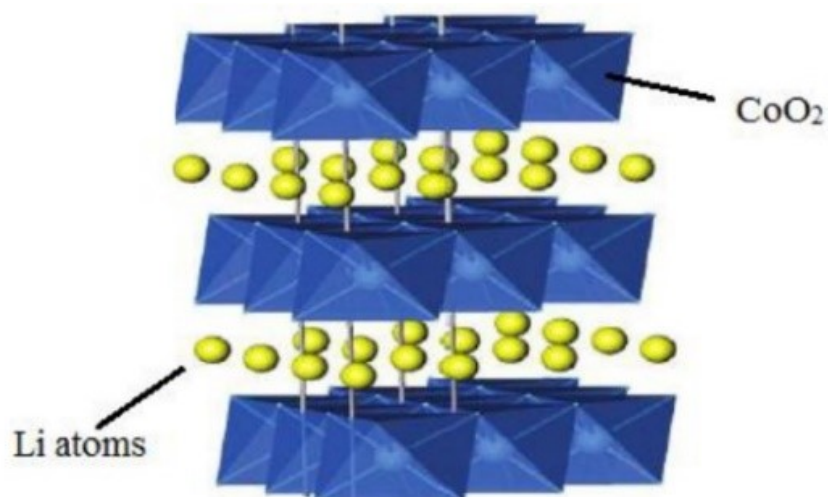


Figure 1.4. Layered structure of LCO [26].

LCO has several desirable features including high discharge potential, low molecular weight, high energy capacity, good charge/discharge performance, relative ease of synthesis and treatment, and stable and high discharge voltage. Despite its high theoretical capacity of 274 mAhg^{-1} , the reported practical discharge capacities of LCO are in the range of $135\text{-}150 \text{ mAhg}^{-1}$ which corresponds to 55-60% of the theoretical capacity. Hence extensive research has been conducted during the last two decades to find cathode materials with larger capacity and higher potential than LCO. Additional factors like high cost, chemical hazards, and the environmental impact associated with cobalt increased the necessity to find novel combinations of cathode material [26, 28].

LMO (LiMn_2O_4) – LMO shared the same early time frame of being proposed as a cathode material in LIBs as LCO. However, its use has not spread mainly due to performance limitations such as low capacity, the difficulty of mass production, and power charge/discharge performance, especially at high temperatures [27]. However, it has been being used as a possible replacement for LCO due to major advantages such as high safety and low cost [27]. The spinel lithium manganese oxide LMO has been one of the most popular cathode materials as a non-toxic, environmentally friendly, high natural abundance of Mn and cost-effective alternative. This material has a theoretical capacity of 148 mAhg^{-1} for an equivalent weight (M) is 180.8 g/mol .

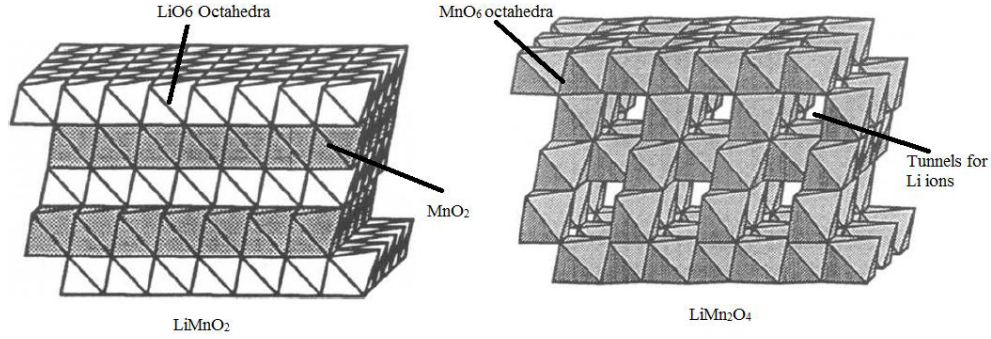


Figure 1.5. Structural comparison between layered LiMnO_2 structure and spinel LiMn_2O_4 structure [29].

A range of synthetic methods similar to LCO has been applied to develop spinel LiMn_2O_4 including solid-state reaction, sol-gel method, hydrothermal synthesis, combustion synthesis, solution-phase, flame-assisted spray technology, and templating method. It was reported that even while LiMnO_2 is synthesized, it tends to revert itself to form a more stable spinel structure LiMn_2O_4 . LMO has proven to be a viable cathode material mainly because of the three-dimensional framework which adds stability to the structure making it a more stable alternative. A range of further derivatives of spinel manganese oxide systems has been studied by researchers to improve structural stability and electrochemical performance. $\text{LiNi}_x\text{Mn}_{2-x}\text{O}_4$ is one of the most prominent derivatives of spinel manganese oxides which shows significant improvement in cycling behavior against that of LMO. These are prepared using techniques like cationic substitution and surface modification [29, 30].

NMC ($\text{LiNi}_{1/3}\text{Mn}_{1/3}\text{Co}_{1/3}\text{O}_2$) – This material was derived from the $\text{LiNi}_{1-y}\text{zMnyCo}_z\text{O}_2$ family group (where $y = z = 1/3$) first published in 1999-2000 [31, 32]. The idea was to mix three transition metals in a certain proportion to take advantage of the properties of all of the elements. Yoshio, the researcher who published it in the year 2000, hypothesized that the addition of cobalt to $\text{LiMn}_{1-y}\text{Ni}_y\text{O}_2$ would stabilize the structure [32]. Mixing these three cations at optimum levels is very important since too much of Co would lead to a decrease in capacity, too much of Ni will result in cation mixing, and too much of Mn can lead to a transformation to the spinel structure.

The layered $\text{LiNi}_{1/3}\text{Mn}_{1/3}\text{Co}_{1/3}\text{O}_2$ was first proposed by T.Ozhuku in 2001 [33] and it has been of great interest and has been extensively researched since then. This combination

has a reversible discharge capacity of about 200mAh/g in the range of 2.5– 4.6V as well as an excellent rate capability and good thermal stability [33]. Studies have also shown that this material, commonly known as NMC111, has better thermal stability compared to the conventional $\text{Li}(\text{Ni}_{0.8}\text{Co}_{0.2})\text{O}_2$ and $\text{LiNi}_{0.8}\text{Co}_{0.15}\text{Al}_{0.05}\text{O}_2$ cathodes [34, 35]. Some of the disadvantages of this material are that its rate capability is not as good as that of LiCoO_2 but is better than that of $\text{LiNi}_{1/2}\text{Mn}_{1/2}\text{O}_2$ and this material is structurally unstable at voltages $>4.6\text{V}$. There are several other combinations like NMC 532 and NMC 622 which are implemented based on conditions and requirements of the battery application.

1.3.3 Degradation and aging mechanisms of LIBs

Degradation of a LIB can be determined based on reduction in usable energy and battery performance. This can be explained using two specific phenomena, capacity loss and resistance rise which also can be referred to as power fade. The capacity loss indicates the irreversible loss of ability of battery to store energy in form of charge. The power fade i.e. resistance rise can be identified as an irreversible reduction in the rate at which electrical energy can be accepted or released by the battery (i.e., fading of power) [36]. In the EV industry, state of health (SOH) is widely used to indicate degradation and a battery is considered EOL when the capacity fades to 80% of initial capacity in high energy batteries while in high power batteries, it is considered when the available power reaches 50% (i.e. 100% impedance increase). Degradation in LIBs occurs throughout the life of battery during charge, discharge, and even rest. The rate of degradation, however, is attributed to several factors including usage, storage condition, and battery chemistry. These factors can be divided into categories such as design, assembly, and application influence. Figure 1.6 represents different factors and modes through which degradation occurs [37].

With a more inside view of a battery, certain physical and electrochemical changes are responsible for this degradation. As shown in figure 1.7, the aging mechanism of the battery can be summarized as loss of lithium-ion inventory (LLI) and loss of anode/cathode active materials (LAM), and difficulties in the movement of lithium ions which indicates an increase in electrical resistance [36]. Furthermore, the battery degradation mode includes the internal resistance increase (RI) and loss of electrolyte (LE). The battery power fade is mostly driven

by a rise in internal resistance also it leads to capacity fade as charge and discharge cut-off voltages remain the same. Loss of additives and electrolytes is another degradation mode as a minor loss in electrolyte can have significant impacts on overall battery performance [37].

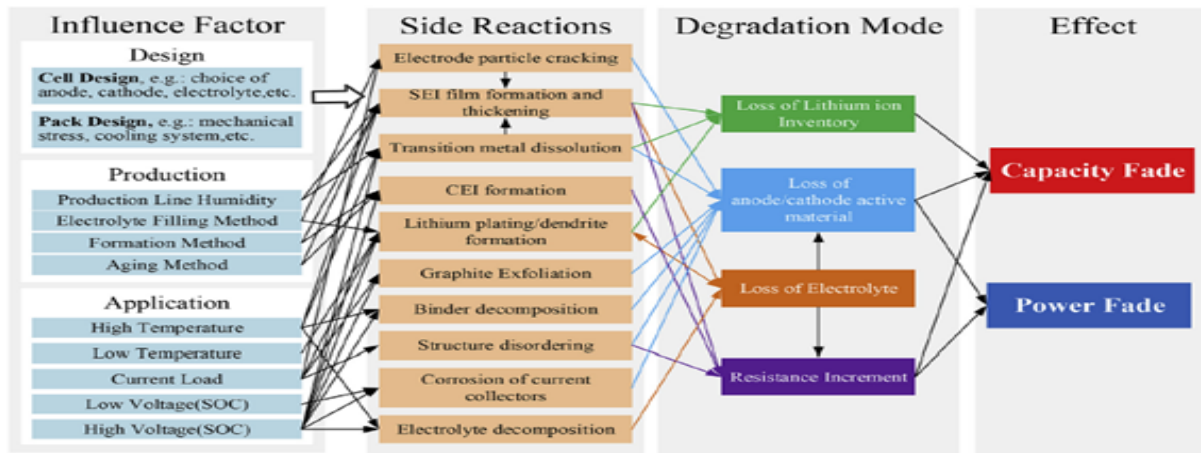


Figure 1.6. Cause and effect of degradation mechanisms and associated degradation modes of typical LIBs [37].

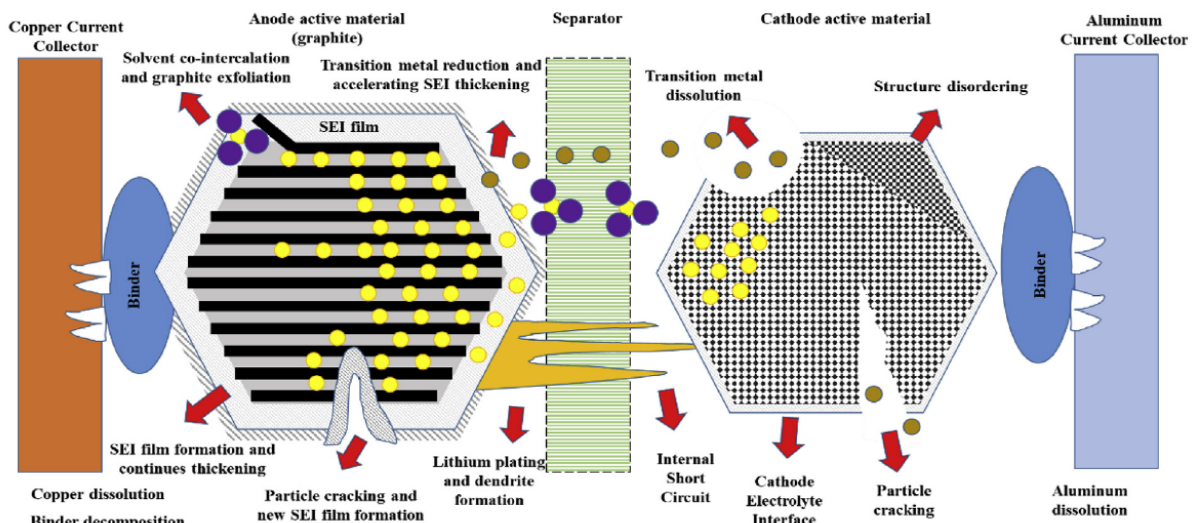


Figure 1.7. Schematic of the main causes of degradation in LIBs [37].

Most batteries used currently show a non-linear degradation pattern throughout their life as indicated in figure 1.8. A fast decrease in capacity is seen in the first few cycles, especially during the first charge which is the result of SEI formation at anode leading to loss of lithium inventory. This also results in a lower coulombic efficiency during initial cycles. In the

second stage, the battery performance fades steadily during its lifetime due to side reactions happening inside the battery as mentioned previously. This stage is mostly the part where the battery is employed for its applications. At the third stage, a rapid capacity loss is seen with a high rise in resistance at end of life. The reason can be due to LLI originated from lithium deposition and LAM [36, 37].

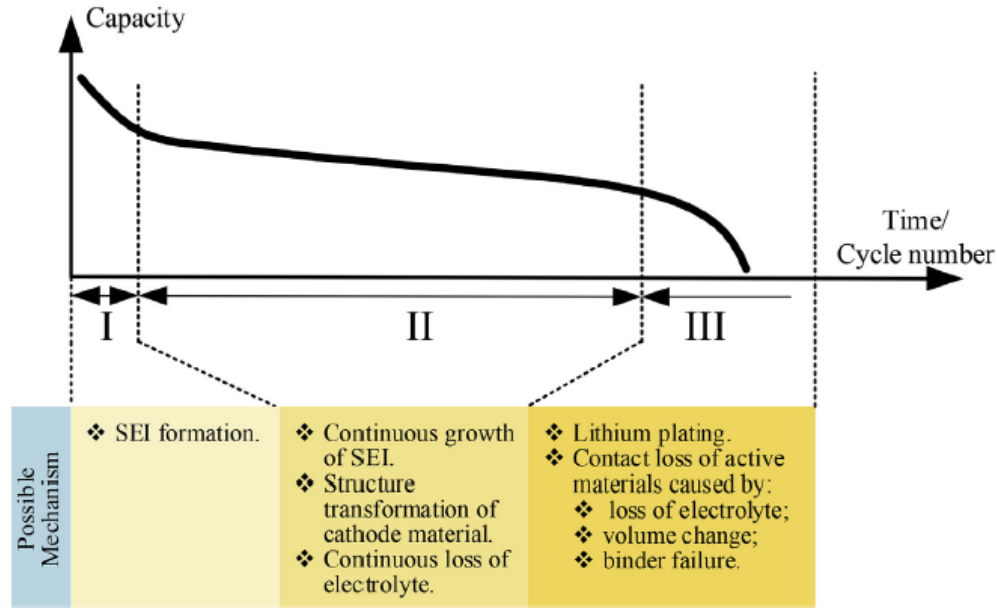


Figure 1.8. Battery capacity fade and possible internal mechanism in different stages [37].

The degradation mechanisms of some cathode chemistries are more frequently than others are discussed in subsequent sections.

LCO Degradation– The capacity fading mechanism of LCO is based on a combination of the structural instability of the layered rock-salt structure and the interface resistance buildup between the cathode and the electrolyte. The effects can be seen in terms of an increase in grain size, decreases in surface potential, and loss of contact stiffness which eventually leads to irreversible capacity fade [38]. Deeper discharge of batteries can also lead to mechanical damage in LCO cathode [39]. Electrical measurements revealed that the cell resistance of a battery with LCO cathode significantly increases with deeper discharges while cycling. Monotonic cycling is considered as another factor causing accelerated degradation of LCO. Mechanical measurements on LCO films revealed that the fracture toughness, the

elastic modulus, and the hardness all decrease by 40 – 70% in samples subjected to a single charge-discharge cycle. These changes can be correlated with microfractures of LCO grains, which is speculated to lead a crack formation and propagation in this material [36].

LCO operates in its specific voltage range and can go up to 4.2 V. Several problems are seen when LCO cathodes are cycled with a higher upper voltage than 4.2V. Three issues associated with higher voltages are considered critical for degradation. Firstly, the interface between the delithiated LCO and the electrolyte is highly unstable at high voltages. The second problem is that co-dissolution increases with a higher cutoff voltage along with the loss of oxygen. The third problem is the degradation of other components such as the binders and the separators which causes detachment of the cathode particles. These factors can cause irreversible surface decomposition and phase transformation of the cathodes, which eventually lead to capacity fade [38].

LMO Degradation– There are several ways in which the degradation process occurs in LMO based cathodes. Mechanisms like phase transformation, Jahn-Teller distortions, mechanical degradation due to crystallinity losses, and dissolution of manganese ions are commonly observed under certain conditions during long term cycling [35]. Cycling at higher temperature at the voltage of 4 V (vs Li/Li+) results in severe capacity fading of LMO. This loss in capacity is explained by Jahn-Teller distortions. These are attributed to acidic environments which cause dissolution of Mn ions from LMO and instable organic electrolytes at higher potentials than 4 V. Deeply discharged LMO electrodes show prominent Jahn-Teller distortions phenomena. Mn ion dissolution over time further contributes to significant capacity fade as well as disturbs the stoichiometry. These effects are further accelerated due to the instability of organic electrolytes at potentials greater than 4 V [40]. Mechanical degradation of LMO also results in a capacity fade. A study reported LMO cathode generates similar microfibers as seen in LCO cases once subjected to cycling which increases over time. The study also demonstrated that irreversible losses in crystallinity after the first charge/discharge cycle and cracks distributed throughout the material’s surface, specifically the (1 1 1) crystallographic plane, and twisted fringes point towards internal stress, leading to microscale structural collapse [41]. TEM studies of LiMn₂O₄ nanowires also showed that fast charging and discharging may cause phase transition regions formed between Li-rich

and Li-poor regions without the presence of fractures in nanowires. While nanowires do not show significant fractures, the cathode material may show an accelerated tendency to form fractures at very high charging rates [35, 41].

NMC Degradation– Large reversible capacities as high as 200 mAh/g can be achieved by incorporating stoichiometric amounts of Mn and Co with Ni, forming a Ni-rich transition metal oxide. Studies on Ni-rich NMC-811 cathodes have reported reversible capacities in the range of 190-200 mAh/g, However, there are certain issues like cycle stability which is associated with many degradation mechanisms. including irreversible structural transformation, thermal degradation, the formation of a cathode electrolyte interphase, and the formation of microcracks in the cathode grains [38].

As different variants of NMC share similar crystal and micro-spherical structures, the majority of the structural degradation mechanisms observed in NMC-based cathodes can be applied to all these variants irrespective of Ni/Mn/Co ratios [38]. However, increasing Ni content for increasing specific energy can also lead to lower cycling stability. An increase in Ni to the relative amount of Ni, Mn, and Co results in the reduced performances as well as other negative features. A study on the NMC-811 sample reported that it had a volume change of 5.1% vs a 1.2% change for NMC-111. The difference in volume change had consequences for structural integrity with the NMC-811 showing more significant microcrack formation and secondary particle disintegration [36].

Other mechanisms of degradation observed in NMC includes 1) phase transformation and the formation of undesirable inactive materials, such as rock salts, resulting in the voltage fade, 2) formation of highly resistive decomposition products due to the exposure of the electrolyte to the high oxidation state of transition metals such as Ni⁴⁺, 3) the blocking effect of the cathode/electrolyte interface, which limits the transportation of Li⁺ back to the cathode, 4) dissolution of harmful metal species such as Mn²⁺ and their migration to the anode side, which could trigger catastrophic solid electrolyte interface formation and consequently trap more active Li⁺, 5) cracking and pulverization of the particles. To summarize, the main cause of capacity fading in NMC is the loss of active Li and the impedance buildup on the cathode side [42].

1.4 Objectives

Currently, LFP and NMC are the two major cathode materials for LIBs, with the respective market share reaching 54% and 42% while LCO remains a major component when it comes to wireless electronics technology. Although there have been several efforts to recycle those cathode materials using direct recycling approaches, most of them have focused on the development of recycling techniques without a fundamental understanding of how direct recycling works. There has been no report on the current challenges of the direct recycling process, such as reproducibility. Thus, it remains unclear whether 1) end-of-life cathode materials can be recycled via a direct recycling approach, and 2) the method can apply to different battery chemistries, and 3) the method can be used for spent cathodes with different levels of degradation.

In this work, we conducted a systematic study on the direct recycling approach starting from liberation/separation of cathode materials from a scrapped battery to cathode regeneration with various processing parameters. The main objective is to investigate the effectiveness of the direct recycling approach and any challenges that we should address for the development of a direct recycling approach.

As the trend in battery manufacturers use a blend of more than one active material components in a cathode depending on the requirement, there is a great interest to know whether the direct approach works for actual mixed cathodes. Therefore, we utilized a combination of NMC and LMO cathode used in Nissan LEAF EVs along with LCO mainly used in electronics batteries. The goal was to develop a loop direct recycling method that can be effectively applied to multiple combinations of battery chemistry by doing modifications in conditions and to gain insight about the effectiveness of these techniques and determine the conditions under which best results are obtained.

Also, a significant argument made in favor of indirect recycling approach is that it is easier to carry out on large scale due to simplicity of process while indirect approach tends to be more complicated. The process flow we used here is easily scalable with the methods of ultrasonication and centrifuge already being employed by industry for various applications while the regeneration processes need only a sealed enclave with no complex steps involved

other than temperature and time monitoring. Additionally, these methods use a fraction of energy and have very less pollutants involved as compared to indirect approach. Successful regeneration using this technique can also solve the objective of developing a scalable technology for regeneration.

This research can give significant insights into difficulties and solutions in dealing with the regeneration of these chemistries and help set up some benchmarking data for future scientific endeavors in this field.

2. EXPERIMENTAL METHODS

2.1 Materials

Cathode materials were extracted from used commercial iPad2 and LEAF EV batteries. A used Apple iPad2 battery, which had minor degradation (less than 5%), includes an LCO-based cathode, confirmed in our SEM/EDAX analysis (Fig. 3.3). A used Nissan LEAF battery, which had cycled to reach its end-of-life (i.e. 20% capacity loss), employs a combination of LMO and NMC due to the individual benefits of these materials. LCO-based batteries have mainly used in electronic devices and their lifespan is in the range of 2-4 years. In contrast, EV vehicles tend to use LMO, NMC, and other alternatives which usually have a lifespan of 7-10 years.

2.2 Recycling process: Cathode Liberation/Separation

We used a multi-step loop approach to liberate and separate cathode active materials from used batteries. We aimed at developing a method to obtain pure cathode active materials, which are free of carbon black and PVDF binder while maintaining crystal structure and chemical composition of cathode active materials. Two different approaches were used to understand the effects of the separation process. One method is a froth flotation-based separation technique which was conducted at Michigan Technological University (MTU) and the other method is an ultrasonication-based separation technique developed and performed in our laboratory. The ultrasonication-based liberation/separation technique involves two steps: 1) cell disassembly and electrode rinsing and 2) cathode active material extraction.

2.2.1 Cell disassembly and electrode rinsing

Once a used battery is discharged up to 2.0 V at a very slow rate, the multi-layered battery was cut open and electrode layers were separated from the separator sheets. As shown in figure 2.1, each electrode sheet was placed in a plastic container containing DMC solution for 3 to 5 minutes for rinsing and the rinsed electrode was further dried completely inside a fume hood. As shown in figure 2.1c, yellowish-golden layer tint was observed due to

residual lithium in anode material. The tint was uneven on anode surfaces which indicates an inhomogeneous SOC (State of Charge) level in each electrode. After drying, the electrode sheets were stored in a vacuum oven at 60 °C overnight. This drying process helps in eliminating any remaining DMC solution used for rinsing or residual moisture.

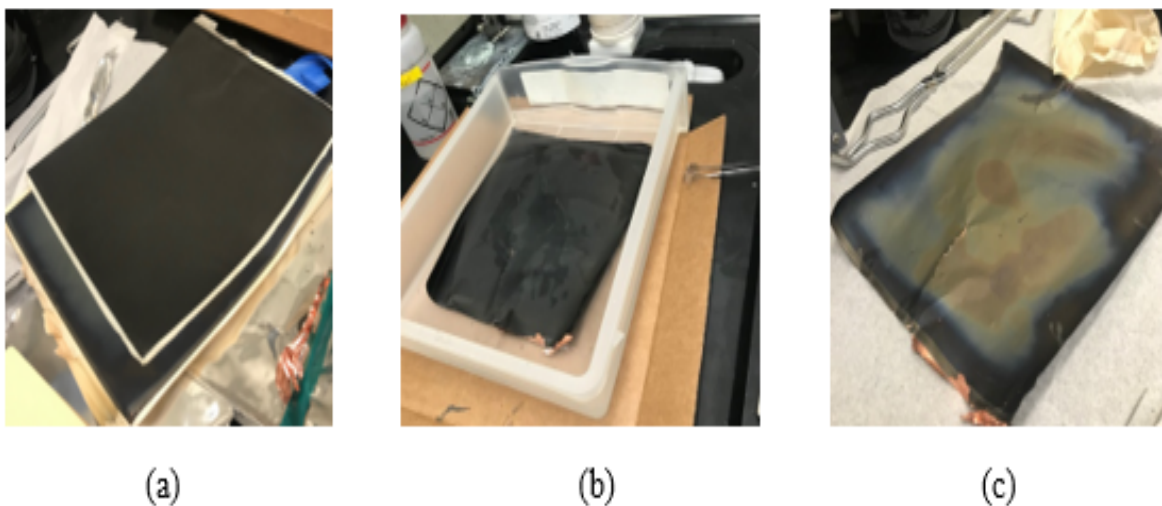


Figure 2.1. The electrode rinsing procedure before cathode material extraction

2.2.2 Cathode material extraction

Organic solvent dissolution technique was used for the separation of cathode black mass from aluminum foil. A rinsed sheet of the cathode was taken out of an oven and cut into small pieces and ultrasonicated at 40 °C for 60 minutes in the presence of an organic solvent, NMP. The PVDF binder used in the cathode was dissolved in NMP while ultrasonication aided the process by loosening the grip of cathode material on the aluminum surface. As shown, cathode materials can be seen to be coming off easily after 60 minutes of ultrasonication (Fig. 2.2a). However, upon carrying out ultrasonication for longer durations, the separated particles may start re-agglomerating due to vibrations in presence of freed binder material in the solution, hence to avoid this, ultrasonication was done for an optimal time of 60 minutes. The obtained solution including cathode black mass was centrifuged. During this process, cathode active materials were deposited at the bottom but lighter materials like carbon particles were suspended in the solution (Fig. 2.2b). Multiple centrifuge processes

(five to six times, 10 minutes each) were carried out using DI water until a clear solution was observed to eliminate carbon additives and light-weight impurities from the black mass if any (Fig. 2.2c). The obtained material was initially dried in a fume hood and then further dried in a vacuum oven at 110 °C to eliminate remaining water used in the process. The resultant powder was grinded in a mortar and pestle and stored inside the vacuum oven again at 60 °C before it is used for battery assembly (Fig 2.2d).

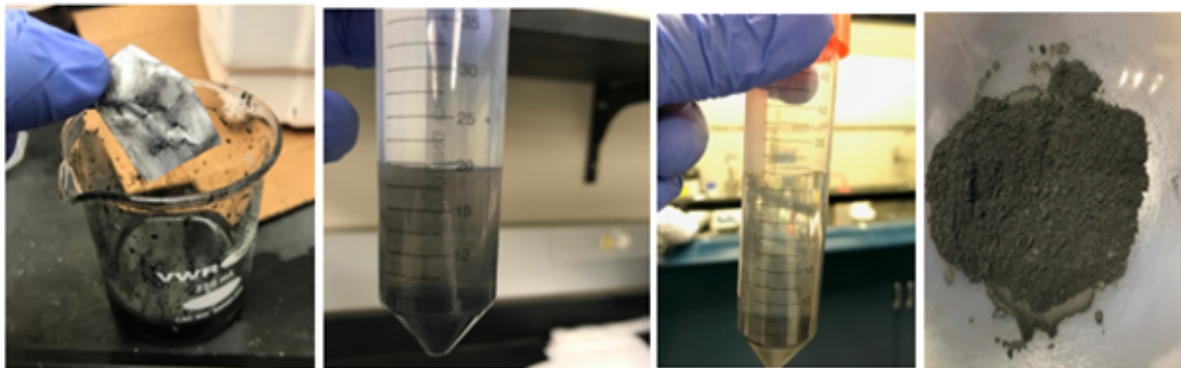


Figure 2.2. The separation process using ultrasonication and centrifuge techniques

2.3 Recycling Process: Cathode Regeneration

Hydrothermal reaction is widely used in the synthesis of various cathode materials and has the capability of generating particles with high crystallinity and desired stoichiometry. The idea is to insert Li into Li-deficient cathode particles found in spent LIBs. In this study, we used methodological steps of hydrothermal synthesis along with heat treatment for cathode regeneration while altering parameters used for the synthesis.

Firstly, we employed hydrothermal regeneration using a closed, titanium high-pressure enclave. A wide range of variations is possible in parameters of hydrothermal synthesis in terms of reaction temperature, cooling temperature, concentration/molar ratio of added lithium salt to active material, reaction time. The process we followed used a specific set of parameters. The separated cathode active material was mixed with LiOH in a molar ratio of 1:1. This material mixture was then added to DI water and the formed solution was placed in a titanium high-pressure enclave reactor in the presence of a magnetic stirrer. The sealed

reactor was placed on a pre-heated heating plate at a temperature of 180 °C with rotations for magnetic stirrer at 1200 RPM and the reaction was carried out for 22 hours. After completion, the reactor was gradually cooled to room temperature before opening. The resulting solution was centrifuged at a high RPM using DI-water to eliminate any excess amount of lithium salt present and further dried in a vacuum oven at 120°C to remove any moisture. Figure 2.3 shows the sealed reactor on the heating plate undergoing reaction and the resultant product after heating under vacuum. The resultant material treated as a regenerated cathode material was used for battery fabrication and testing.

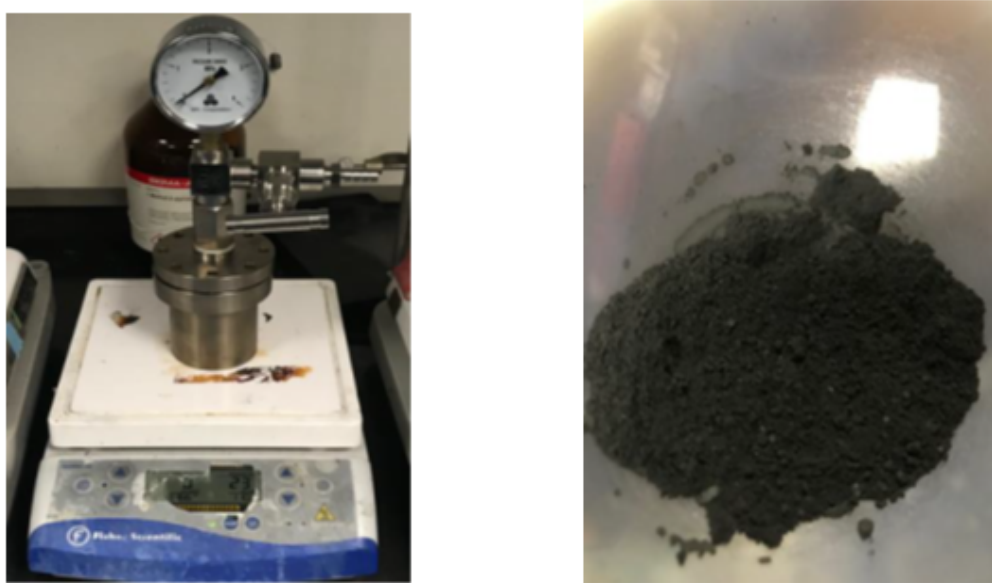


Figure 2.3. Hydrothermal reaction: a) hydrothermal reactor setup; (b) final product after synthesis.

Based on the observed results, process modification was made to tackle certain issues with electrochemical cycling and improve overall results. The first change was done in changing of water to solvent. As the hydrothermal process may damage some aspects of active material, water was replaced with Triethylene glycol (TEG). Replacing TEG was the only alteration done in this set of regeneration while keeping other parameters identical to understand the effects of solvent used in the process. This process was named solvothermal synthesis. Another alteration was done in terms of the molar ratio of active material to LiOH as the performance observed in solvothermal synthesis was significantly improved yet shorter

in terms of expected regeneration effects. Several studies suggested that molar ratio has the most significant impact on regeneration compared to any other parameter [47,49,50]. Most studies were conducted with molar ratios ranging from 1:1 to 1:10 or more. In our work, a molar ratio of 1:5 between the active material and LiOH was used which signifies increasing lithium salt concentration, i.e., availability of more lithium to be replaced in delithiated lattice of active material. Other parameters of synthesis, fabrication, and testing were kept identical.

We also investigated a heat treatment step applied after the hydrothermal reaction process. The regenerated cathode powder outcome of hydrothermal process was subjected to heat treatment at high temperatures of around 550-600 °C. A ceramic container carrying the powder was placed in a heating furnace with a pre-defined heating program and heat-treated in between 4-7 hours depending on the requirements of the process. Figure 2.4 shows the furnace with a specific heating program as used in this study.



Figure 2.4. A furnace used for heat-treatment process.

2.4 Material Characterization: SEM/EDS, ICP, XRD, and TGA.

Various characterization techniques are used to understand the structure and composition of active material and to analyze the effects of various parameters used in the development of a regeneration process. These techniques are very helpful to predict the performance and understand the causes behind it. X-Ray diffraction (XRD), Inductively Coupled plasma-optical emission spectroscopy (ICP-OES), Scanning electron microscopy (SEM) along with energy dispersive X-ray spectroscopy (EDAX), Thermogravimetric analysis (TGA) were used in this study.

2.4.1 Scanning Electron Microscopy (SEM)

SEM is one of the indispensable tools for the characterization of materials ranging in nanometer to micrometer scale. The versatility of the method allows it to be used for the examination and analysis of the microstructure morphology and chemical composition. SEM uses a focused beam of high-energy electrons to generate a variety of signals at the surface of solid specimens [51]. Figure 2.5 shows the schematic of the structure and working of a scanning electron microscope. The principle of operation of SEM is based on the fact that accelerated electrons in an SEM carry significant amounts of kinetic energy. This energy is dissipated when the incident electrons are decelerated in the solid sample and a variety of signals are produced by electron-sample interactions. Secondary electrons are responsible for producing SEM images, backscattered electrons (BSE), diffracted backscattered electrons, photons as characteristic X-rays that are used for elemental analysis, visible light, and heat. Backscattered and secondary electrons are commonly used for imaging samples. Secondary electrons provide information about morphology and topography on samples and backscattered electrons are used for illustrating contrasts in composition in multiphase samples with rapid phase discrimination. This instrument can also be used in association with other related techniques like EDAX for the determination of the composition or orientation of individual crystals or features.

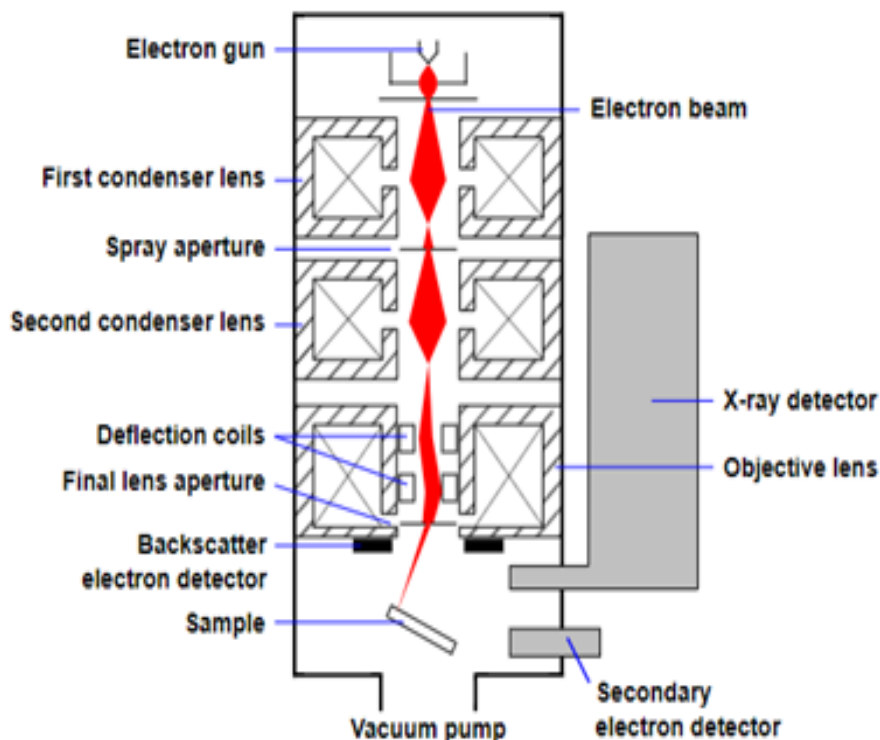


Figure 2.5. Schematic of SEM

SEM/EDAX analysis was conducted after both liberation and regeneration steps to obtain information such as texture i.e. external morphology, chemical composition, and crystalline structure, and orientation of material ingredients of the sample. Materials liberated from cathode were examined for the formation of cracks and broken/disturbed crystalline structure which is common during long-term cycling and might also occur during the liberation process.

Furthermore, it was used to examine any impurities present such as carbon black on separated cathodes. Materials with no significant change in crystalline structure and the absence of impurities indicate the effectiveness of the separation process. SEM was also carried out after regeneration synthesis. Any morphological changes occurring due to the re-lithiation process were evaluated. Figure 2.6 shows an SEM image of a synthesized sample at IUPUI.

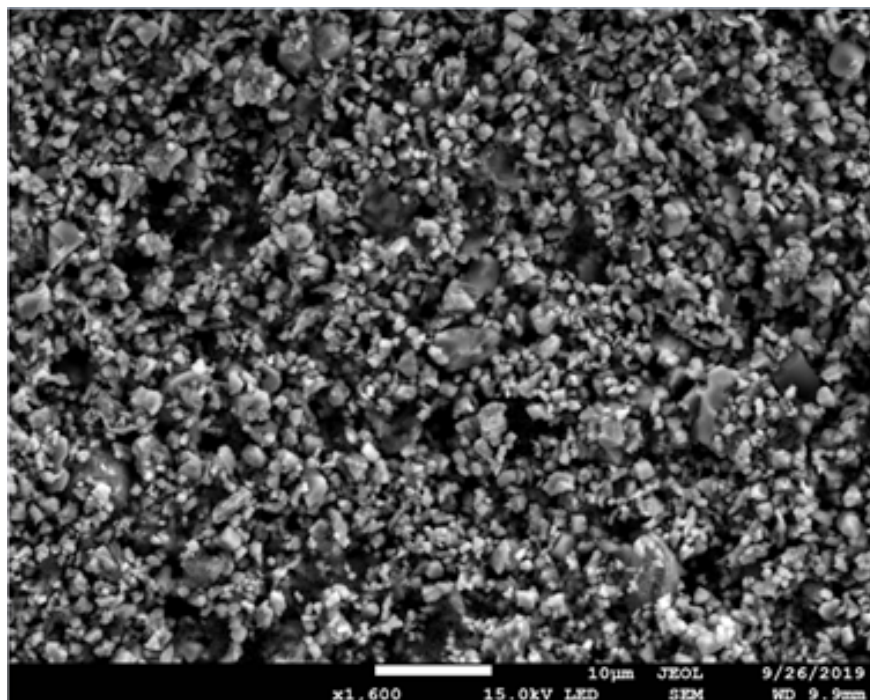


Figure 2.6. An SEM image of a hydrothermally synthesized cathode material (Performed at IUPUI)

2.4.2 X-Ray Diffraction (XRD)

XRD is a popular crystallography technique used for the prediction of composition and molecular structure of a material sample. It is widely used in research for material characterization to understand the effects different processes have on molecular structure, grain size, residual stresses generated in electrode materials. Comparing the samples with virgin materials helps to determine degradation and effects or regeneration processes. XRD works on the principle of Bragg's which provides a way to determine crystal structure based on the angle of reflection of X-Ray beams along with a relation between wavelength and angle of reflection, $n\lambda = 2d\sin\theta$. The variable d is the distance between atomic layers in a crystal, and the variable λ is the wavelength of the incident X-ray beam. XRD data help to distinguish the structure and composition of constituent materials in a sample [52]. Figure 2.7 shows a typical modern XRD setup and figure 2.8 shows the working principle behinds XRD operation.

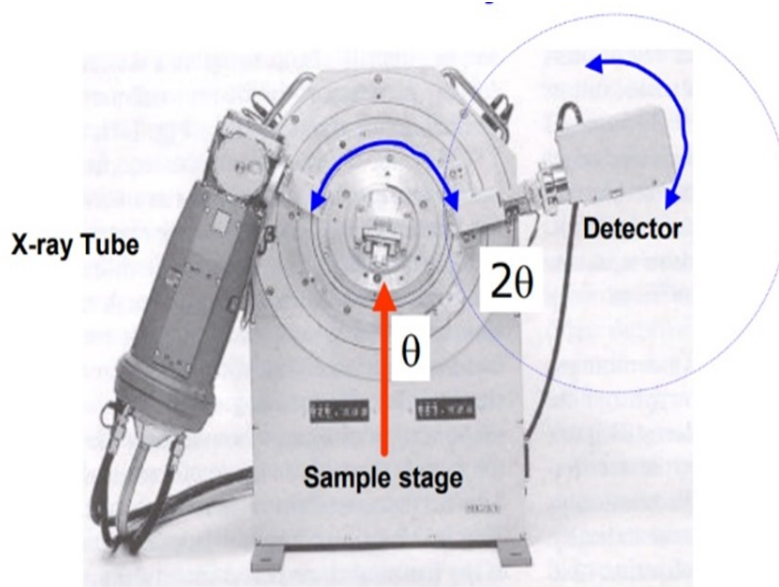


Figure 2.7. A Modern Automated X-ray Diffractometer

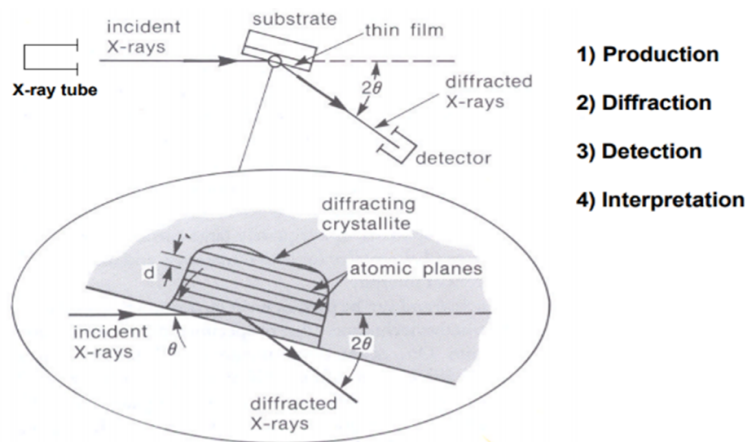


Figure 2.8. Working principle of an X-ray Diffractometer

Repetitive cycling, heating processes, and regeneration processes can potentially lead to different structural and chemical composition along with the formation of undesired phases. We performed XRD analysis to understand potential undesired phases after cathode regeneration, along with any changes in phases or structures caused by a regeneration process. It

was also used for determining the effectiveness of our separation/liberation technique. We inspected the success regeneration methods by comparing XRD patterns of virgin materials and regenerated materials.

2.4.3 Inductively coupled plasma-optical emission spectroscopy (ICP-OES)

ICP-OES is an elemental analysis technique used to measure the concentration of certain material present in the liquid or solid samples. In ICP-OES, a plasma (a gas containing a significant number of ions) is formed by passing a neutral gas such as argon, through a plasma torch with electrons. An intense electromagnetic field is created within the coil when the torch is turned on. The ignited argon gas flowing through the torch initiates an ionization process which is further intensified by colliding electrons. A sample to be tested is introduced in the form of atoms through a nebulizer in this plasma. Ionization due to high energy electron collision followed by inevitable deionization occurs resulting in atoms emitting packets of energy characteristic to their formation. The wavelength of this energy is used to precisely determine the presence of elements in the sample. Different emitted wavelengths and colors are measured using an array of semiconductor photodetectors and are used by ICP-OES to predict the constituent element [53]. Figure 2.9 shows the ICP-OES apparatus used for this research at IUPUI.

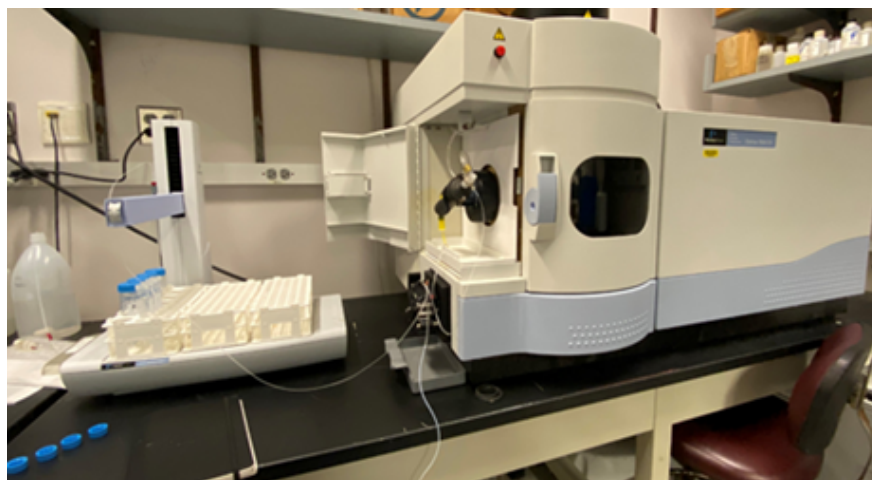


Figure 2.9. ICP-OES instrument used for this study

Digesting the powder sample in strong acids is a prerequisite for conducting ICP. As powdered samples cannot be tested for ICP as it is, they are digested in concentrated acids. Once the materials are completely dissolved in the acids, these acid-material solutions are diluted using DI water by a ratio ranging from 1:10 up to 1:100 depending on the molarity of acid used. These diluted solutions are the final product of digestion and can be used as precursors for ICP. Digestion is a very important step such that incomplete digestion can result in the false composition of data leading to misinterpretation of sample defying the purpose of whole ICP tests. After several trials with and without microwave assistance, we developed the most effective technique. An equal amount of high concentration HCL and H₂SO₄ acids were mixed in a plastic container and the sample was added to it to be left overnight. We found this combination to be most reliable for digestion.

ICP-OES was carried out to understand whether lithium can be reinserted into cathode during a regeneration process. ICP measurements of the materials before and after undergoing lithiation were taken and compared to see an increase in the relative weight of lithium to inspect the effectiveness of the regeneration process.

2.4.4 Thermogravimetric Analysis (TGA)

Thermogravimetric analysis also referred to as thermal gravimetric analysis (TGA) is a method of thermal analysis that monitors the mass of a substance as a function of temperature under a controlled environment. TGA can help understand physical phenomena, such as phase transitions, absorption, and adsorption; as well as chemical phenomena including thermal decomposition, and solid-gas reactions such as reduction and oxidation. A thermogravimetric analyzer is used to conduct TGA which consists of a sample pan supported by a precision balance and a heating furnace arrangement. A purge gas is used which essentially can be inert or a reactive gas depending on the objective of the experiment. The gas is made to flow over the sample and exits through an exhaust which helps controls the sample environment. The changes in the mass of material are precisely monitored as it is heated in a pre-defined manner using the furnace over time. The results indicate the precise mass of loss associated with a certain temperature to understand the thermal stability [54]. Figure 2.10 shows the schematic of a typical thermogravimetric analyzer.

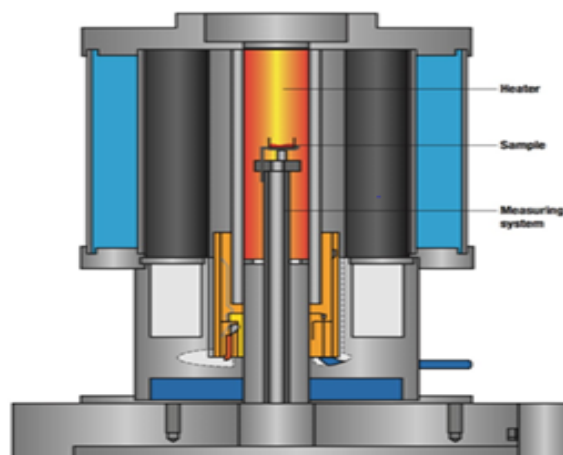


Figure 2.10. Schematic of a typical thermogravimetric analyzer

TGA is used as a method for materials characterization through the analysis of characteristic decomposition patterns of materials at higher temperatures. In this work, it was utilized to inspect the thermal stability of degraded materials, as well as to check any remaining impurities in the recycled sample like carbon additive. Figure 2.11 shows a typical TGA curve, which was obtained at IUPUI.

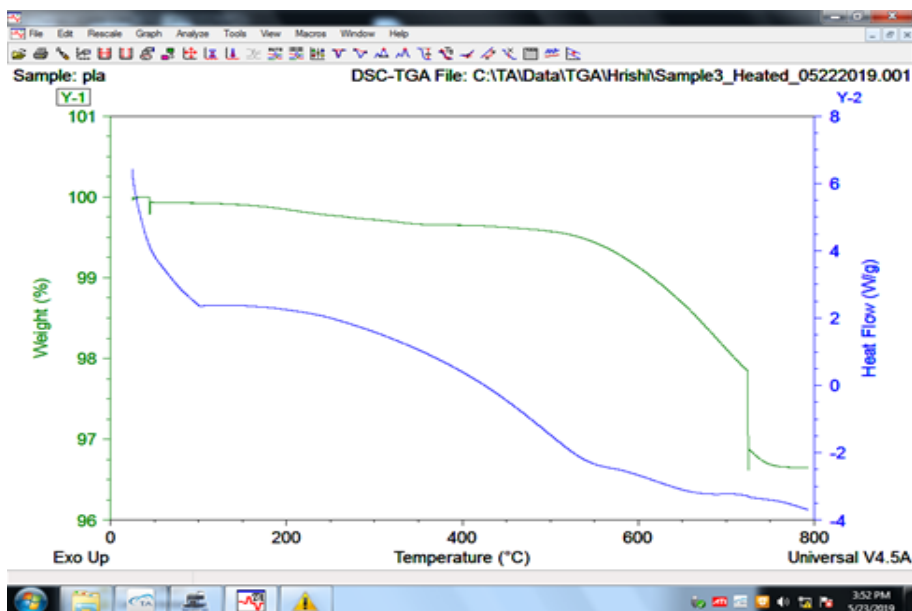


Figure 2.11. A typical nature of the TGA curve

2.5 Battery Electrode Fabrication

2032-coin cells were made in a half-cell configuration (cathode vs. Li) to evaluate the electrochemical performance of recycled cathode materials. The overall process of making and testing coin cells can be divided into three distinct stages: 1) electrode fabrication, 2) coin cell assembly, and 3) testing.

2.5.1 Electrode Fabrication

Firstly, the cathode active material was mixed with precise amounts of carbon additives to improve performance along with a binder. The formation recipe used consists of 90% cathode active material mixed with 1 % KS6 L graphite and 3% C65 carbon black additives, and 6% PVdF binder. The mixture is transferred in a glass container and some amount of NMP solution is added to it. This glass container with the mixture is transferred on a stirring plate with a magnetic stirrer. The mixture is stirred at 1200 RPM for 8-10 hours to form a uniform blend of materials. The mixed slurry is coated on a current collector aluminum foil. The thickness of the coating depends on the desired thickness of the electrode. After coating, the electrode is placed inside a vacuum oven at 110 °C overnight. This effectively eliminates all the NMP solution, giving a solid electrode active material coat on the surface of aluminum foil. Small round electrodes are punched out of this form electrode sheet to be used in coin cell fabrication. To improve wettability and acquire uniform thickness across the electrode, the sheet is calendared using a calendaring apparatus with pre-defined thickness. The electrode is stored either in the vacuum oven or an argon-filled glove box before cell fabrication to ensure that no damage would cause the material by air and moisture. Figure 2.12 shows a coated electrode fabricated and a batch of punched out coin cell cathodes from the coated cathode sheet.

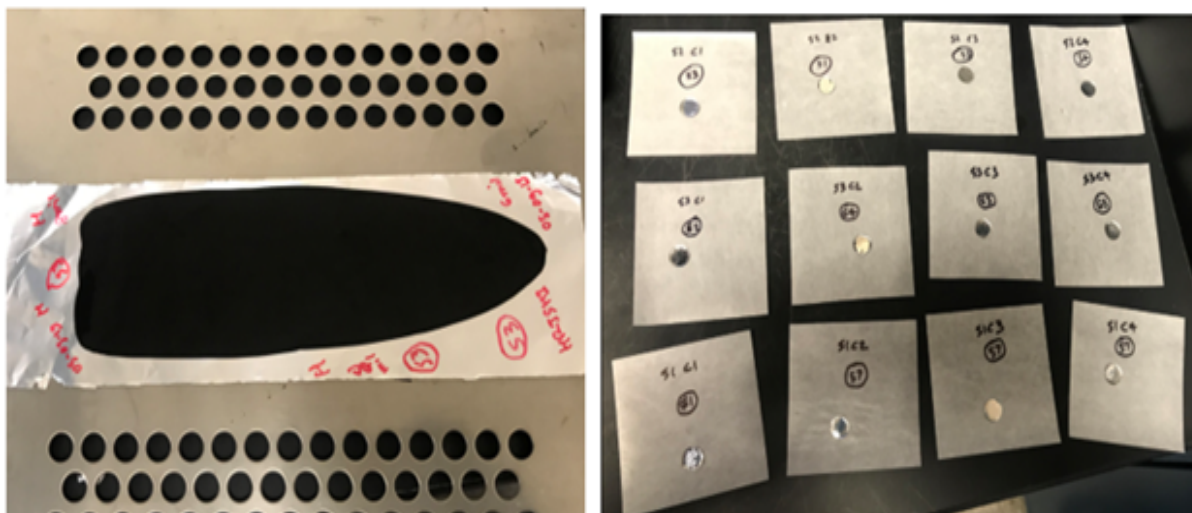


Figure 2.12. Coated cathode on aluminum foil (a) and a batch of coin cell cathodes punched out of it at IUPUI (b)

2.5.2 Coin cell assembly

A half-cell is used for cathode material testing. Firstly, the active material cathode is placed at the bottom shell with its active material side facing up. Some amount of LiPF_6 containing electrolyte is added to the surface of this electrode. After adding the electrolyte, a lithium metal electrode is used on the other side as the reference electrode. After the electrode, a stainless-steel spacer and spring combination are added to the top of this sandwich structure. At the end, the top shell, a bit smaller in diameter compared to the bottom shell, is added on the top of this structure, and is sealed by a locking mechanism of press-fit using a mechanical pressure gauge. Figure 2.13 shows the architecture and orderly steps involved in coin cell assembly. The coin cells are assembled in an argon-filled glove box under a controlled environment to ensure the absence of moisture, air, and other impurities. These cells are checked for open-circuit voltage (OCV) and are kept as it is for a few hours to ensure good surface wetting before being subjected to electrochemical cycling and testing [55,56].

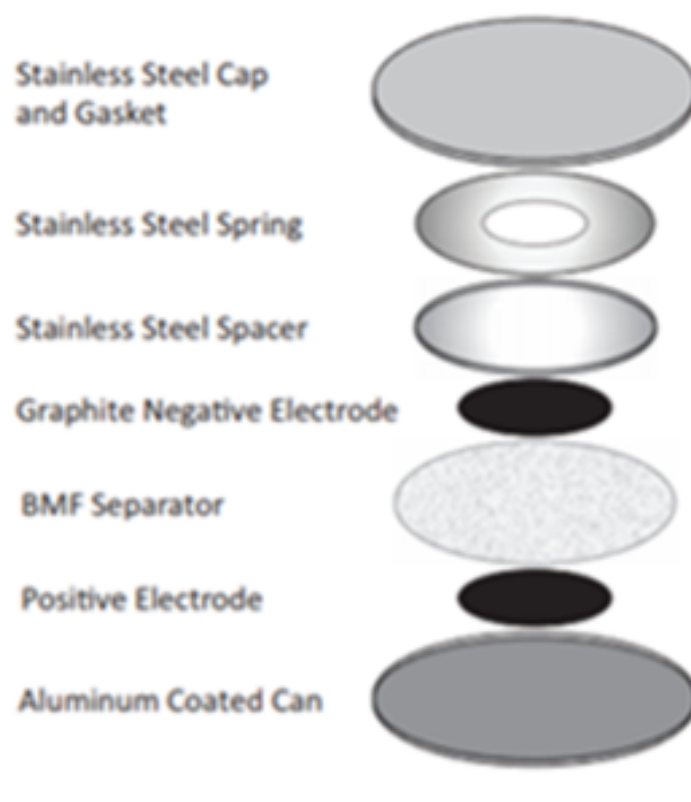


Figure 2.13. Architecture and assembly of a typical coin cell [56]

2.5.3 Coin cell Testing

The fabricated battery cell is tested to evaluate the electrochemical performance of recycled cathodes. Firstly, an operating voltage of the cell is determined, which depends on the characteristic of active material chemistry used. For the cathode materials we used, 3-4.2 V is considered as an optimal voltage range [57]. The cell was cycled at a rate of C/10. The C-rate of C/10 (i.e., 0.1C) signifies that a charge cycle and a discharge cycle will take 10 hours individually at a theoretical capacity value. Along with C-rate and charge-discharge cut-off voltages, certain other parameters such as resting time and charging /discharging protocols, and the number of cycles is pre-defined using a scheduler program. Figure 2.14 shows the ‘constant current-constant voltage charge (CC-CV) and constant current discharge’ protocol used for cycling cells in this research. Figure 2.15 shows the ARBIN and 8 channel MTI setup used for the electrochemical cycling of cells for this research at IUPUI.

1	OCV	2	Rest				
	Log Limit	Step Limit	Goto Step	Variable1	Operator1	Value1	
1	✓	✓	Next Step	PV_CHAN_St	>=	02:00:00	
2	✓	✓		DV_Time	>=	00:30:00	
2	Charge_CC	3	C-Rate	0.1			Lo
	Log Limit	Step Limit	Goto Step	Variable1	Operator1	Value1	
1	✓	✓	Next Step	PV_CHAN_Vo	>=	4.2	
2	✓	✓		DV_Time	>=	00:00:30	
3	✓	✓		DV_Voltage	>=	0.01	
3	Charge_CV	2	Voltage(V)	4.2			Lo
	Log Limit	Step Limit	Goto Step	Variable1	Operator1	Value1	
1	✓	✓	Next Step	PV_CHAN_Cu	<=	0.13	
2	✓	✓		DV_Time	>=	00:00:10	
4	Rest1	2	Rest				
	Log Limit	Step Limit	Goto Step	Variable1	Operator1	Value1	
1	✓	✓	Next Step	PV_CHAN_St	>=	00:10:00	
2	✓	✓		DV_Time	>=	00:00:10	
5	Discharge_C	3	C-Rate	-0.1			Lo
	Log Limit	Step Limit	Goto Step	Variable1	Operator1	Value1	
1	✓	✓	Next Step	PV_CHAN_Vo	<=	3	
2	✓	✓		DV_Time	>=	00:00:30	
3	✓	✓		DV_Voltage	>=	0.01	
6	Rest2	2	Rest				
	Log Limit	Step Limit	Goto Step	Variable1	Operator1	Value1	
1	✓	✓	Next Step	PV_CHAN_St	>=	00:10:00	
2	✓	✓		DV_Time	>=	00:00:10	
7	Loop	2	Set Variable(Reset	Increment	Decrement	
	Log Limit	Step Limit	Goto Step	Variable1	Operator1	Value1	
1	✓	✓	Charge_CC_C	PV_CHAN_Cy	<=	5	
2	✓	✓	End Test	PV_CHAN_Cy	>	5	

Figure 2.14. A CC-CV protocol between 3-4.2 V at a rate of C/10 used for initial cell cycle tests at IUPUI

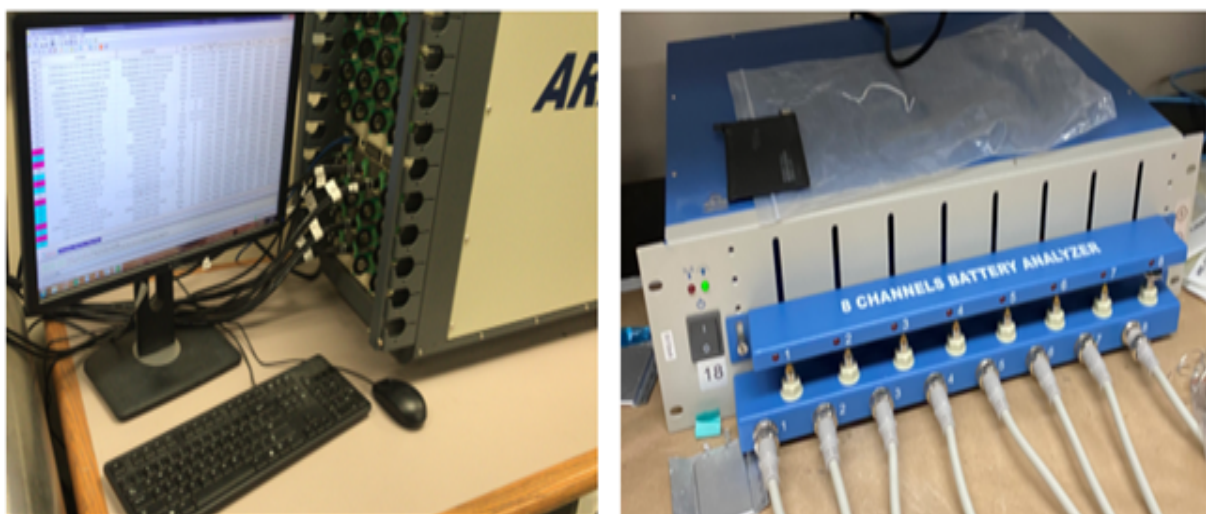


Figure 2.15. ‘ARBIN’ and ‘MTI 8-channel’ cell cycler setups used for cell testing in this research at IUPUI.

3. RESULTS AND DISCUSSION

3.1 Separation effects (Ultrasonication vs. froth-flotation)

Liberation/separation is a vital step in the process of cathode regeneration or recycling. The capacity and long-term cycling ability of the extracted cathode material depends on the effectiveness of employed separation techniques. We developed an ultrasonication-based technique for material liberation/separation along with studying froth flotation technique carried out at Michigan Technological University (MTU) to get a comparative insight on the effectiveness of the ultrasonic technique employed. The plots and discussion in the subsequent results section with the title as ‘MTU sample’ represent the various testing data for samples and cells made out of this froth flotation experiment carried out at MTU while the data titled as ‘IUPUI sample’ represents that of in house ultrasonication separation experiment.

The technique applied involves two distinct steps for liberation/separation which include ultrasonication in the presence of NMP solvent followed by a centrifuge process. The purpose of ultrasonication is to assist in liberating cathode materials from aluminum current collector and separate cathode active material from cathode materials (i.e., active material and carbon black), while the centrifuge process facilitates the material separation further based on the difference in material density. Figure 3.1 shows the liberation process via ultrasonication. As shown, cathode materials including active material and carbon black were successfully liberated from the current collector, while PVDF binder was dissolved in NMP solution.

Separation of cathode active material and carbon black was performed via the centrifuge process. Lightweight carbon black particles can be eliminated using centrifuge as they are suspended in solution while heavy active materials settle at the bottom during centrifuge. Running centrifuge multiple time maximizes the chances of the complete elimination of carbon black and impurities. Figure 3.2 shows the separation and elimination of impurities during multiple runs of the centrifuge.

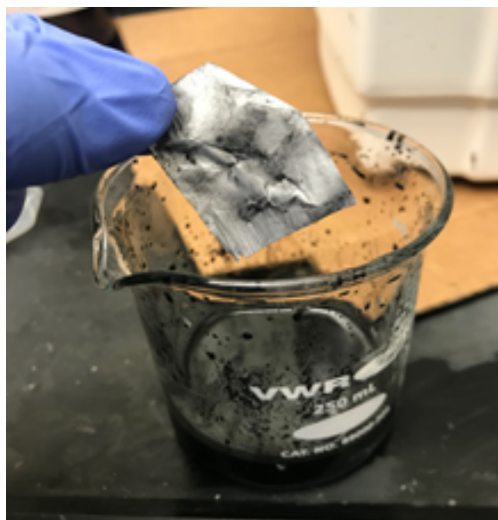


Figure 3.1. Liberation of cathode active material from aluminum foil as a result of ultrasonication

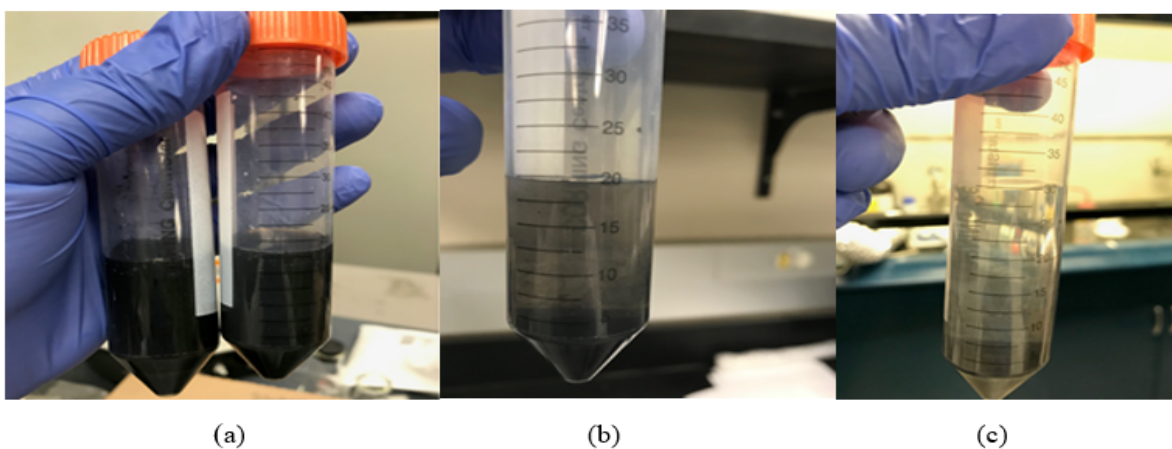


Figure 3.2. Different stages of removal of impurities using centrifuge: a) initial stage before centrifuge, b) after 1st centrifuge run, and c) 5 runs of the centrifuge

The key to a successful liberation/separation process is to keep the structure and chemical composition of cathode active material intact during the process [58]. The effectiveness of our ultrasonication-based liberation/separation technique is discussed further based on morphology, purity, chemical composition, and electrochemical performance.

3.1.1 Morphology and purity: SEM/EDAX characterization

SEM can be used to gain insights into the morphology and material structure of materials, while EDAX can provide elemental analysis of materials. Previous studies have reported the usability of SEM/EDAX in the determination of the presence of impurities in separated cathode materials [58]. First, we performed SEM/EDAX analysis on the cathode separated from iPad2 using a combination of ultrasonication and centrifuge to investigate the purity of the separated material. As shown in figure 3.3, the EDAX spectrum displays only Co and O elements that originate from LCO active material, demonstrating the effectiveness of our ultrasonic-based separation technique. The result confirmed that carbon black and PVDF binder were successfully separated from the cathode and only LCO cathode materials remained after the ultrasonication-based separation process.

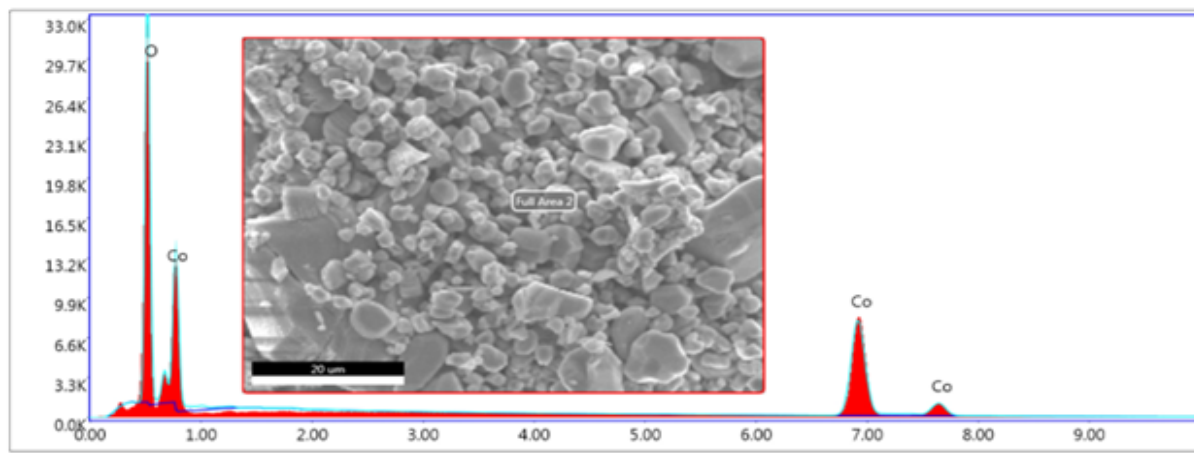


Figure 3.3. EDAX spectrum with the corresponding SEM image of cathode extracted from iPad2 cell using an ultrasonication-based separation technique

We also performed SEM analysis on the material extracted from LEAF cells to investigate the morphology and compared it with that of a material extracted using thermal treatment [58]. Figure 3.4 shows the comparison of cathode active materials separated by (a) heat treatment and (b) ultrasonication.



Upon closely analyzing the SEM images, notable differences can be found. As shown in figure 3.4a, the cathode material liberated/separated via heat treatment for separation/liberation process showed a significant number of agglomerated particles, which presents in the forms of large particles or chunks. This may indicate the presence of PVDF binder after the heat treatment process, leading to significant particle agglomeration. In contrast, a much smaller particle size and a larger specific surface area can be seen in the cathode separated by an ultrasonication-based technique (Fig 3.4b). This is the result of the dissolution of PVDF in NMP solution and dispersion of cathode particles during ultrasonication which leads to a decrease in the degree of agglomeration in the material. Besides, no visible crack formation

can be seen on active material particles suggesting that the material remains intact after the separation process. Carbon black is also hardly observed in the material separated by the process. Hence, SEM analysis suggests that impurities (i.e., PVDF binder and carbon black) are largely eliminated with the decrease in the degree of agglomeration while keeping the morphology mostly unaffected during the ultrasonication process.

3.1.2 Chemical composition: ICP characterization

ICP-OES is a versatile technique to investigate the chemical composition of a material. This technique was used to understand if there are any changes in the chemical composition of a material occurring during the separation process. To evaluate the reproducibility and effectiveness of our liberation/separation process, we also compared the results of ICP analysis generated for ultrasonication and froth flotation samples. We ran two samples of each of IUPUI ultrasonication materials and MTU froth flotation materials. The samples represent materials extracted from Nissan LEAF cells separated using froth flotation for ‘MTU samples’ and ultrasonication for ‘IUPUI samples’ Figure 3.5 represents the relative weight of the chemical elements in different samples.

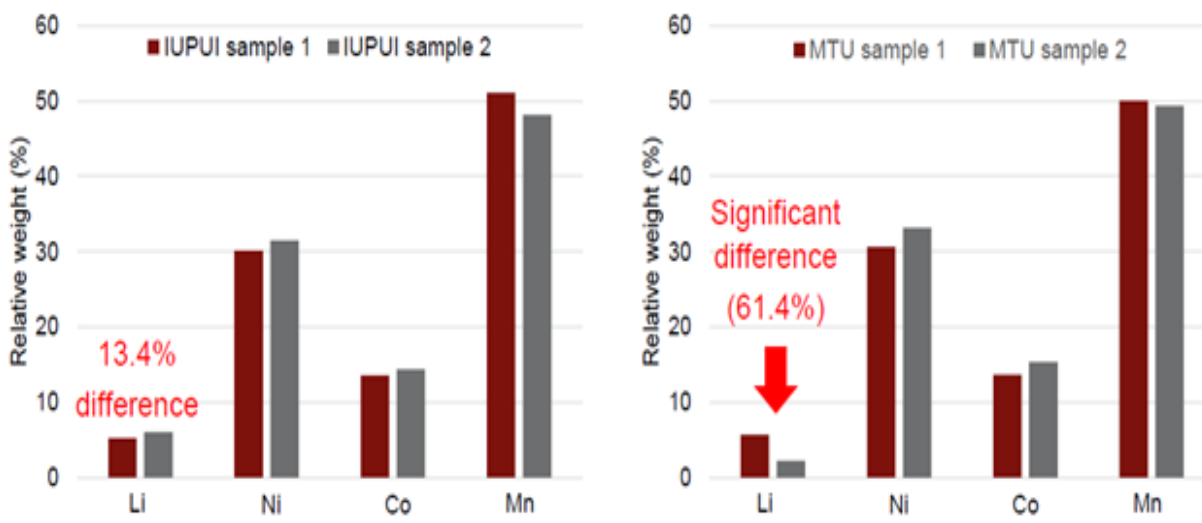


Figure 3.5. Relative weight of constituent materials measured by ICP

As seen in figure 3.5, both samples extracted using ultrasonication indicate similar relative weight and ratio across constituent metals. Only about 13% variation in the relative weight of lithium across two samples was seen. This small difference could be a result of inhomogeneous delithiation of the cathode in the spent Li-ion battery. However, in the case of froth flotation samples, more than 61% of the change in the relative weight of lithium was seen. Multiple factors can be responsible for such a drastic difference. One of the main reasons is the exposure of cathode material to a large amount of water during froth flotation. Some cathode materials are sensitive towards exposure to moisture and air, and thus delithiation of the cathode may occur upon exposure to water during the process. Considering that both processes used a cathode extracted from the same battery with the only difference being in separation techniques, it can be concluded that a loss of lithium inventory in cathode may occur during froth flotation process. Hence, given the better consistency in terms of maintaining the chemical composition and negligible, if any, loss of lithium inventory, the developed ultrasonication-based technique is proved to be an effective approach for liberation/separation of cathode materials.

3.1.3 Electrochemical performance

To investigate electrochemical characteristics of separated cathode active material, an initial cycle test was performed. As shown in figure 3.6a, the discharge capacity of the separated cathode was close to 95 mAh/g (in the range of 80 to 95 mAh/g for multiple samples). Considering the degradation level (20%) of LEAF battery used in this study which has an estimated capacity in the range of 120-130 mAh/g in new condition, the observed capacity was reasonable. This also confirms that there was no significant loss of lithium in the cathode during the ultrasonication-based separation process.

However, with the standard constant current-constant voltage CC-CV protocol, a high CV charge capacity was observed in the first cycle, indicating a high internal resistance during the first charge. To determine whether this was due to the separation process or the nature of the severely delithiated material, a comparative study was carried out with a used iPad2 cell with minor degradation.

Figure 3.6 shows the charge-discharge curves of the initial 2 cycles for separated materials from Nissan LEAF and Apple iPad2 cells using the identical ultrasonication approach performed at IUPUI.

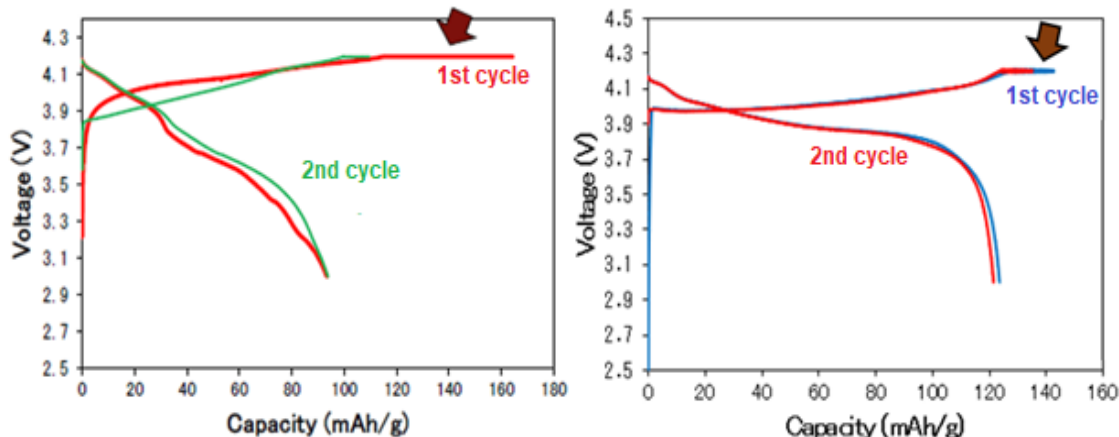


Figure 3.6. The 1st and 2nd charge-discharge curves of cathodes recycled by ultrasonication separation from (a) Nissan LEAF cell (20% degraded) and (b) Apple iPad2 cell (minor degradation)

It was found that the high CV charge capacity seen in the 1st cycle of the LEAF sample did not appear in the iPad2 sample. Upon testing multiple samples, similar results were seen. As both samples were separated using the identical method, it proves that the high CV charge capacity seen in the LEAF sample cannot be attributed to the effect of the separation process. Rather, it could be a result of a property of the cathode chemistry or degradation level. The LEAF cathode is composed of NMC and LMO and it was obtained from a 20% degraded EOL battery. However, the iPad cathode is made up of LCO and the iPad2 battery was slightly degraded (less than 5%).

To investigate how different methods of separation can affect the electrochemical performance of the cathode material, we compared the electrochemical performance of the cathode materials separated using IUPUI's ultrasonication method and the froth flotation method carried out at MTU. Figure 3.7 represents the charge and discharge curves of cathodes separated by using ultrasonication and froth flotation methods under identical conditions and protocols.

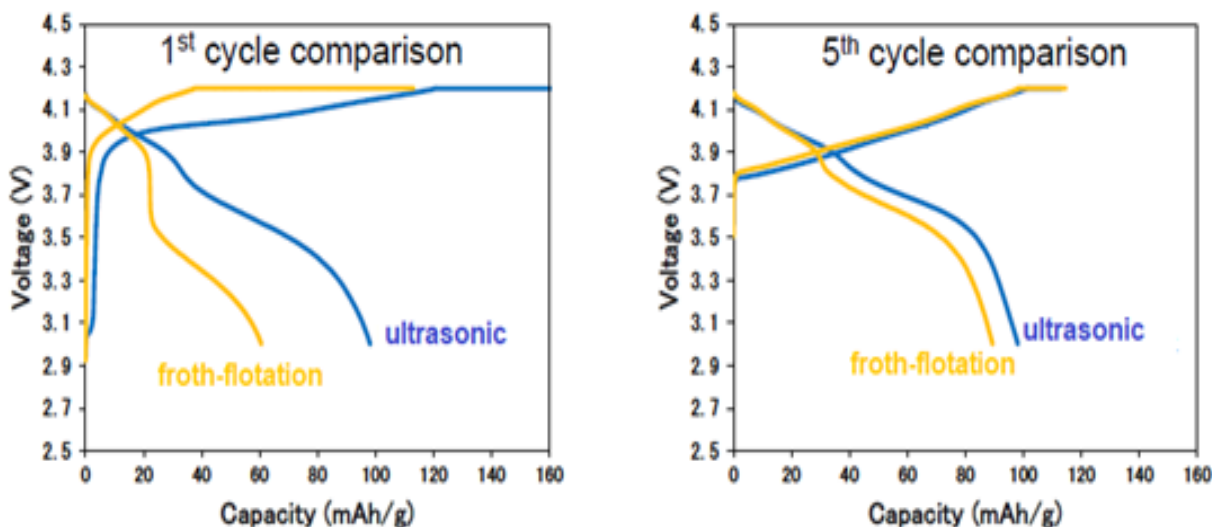


Figure 3.7. The charge and discharge curves for the 1st and 5th cycles of cells with cathodes separated from ultrasonication and froth flotation techniques

The result shows that there are differences in the initial cycle characteristics of ultrasonic- and froth flotation-processed samples. The lower capacity and overpotential were seen for the froth flotation sample in the 1st cycle, suggesting inferior characteristics compared with the ultrasonic sample. This could be due to the usage of water in the froth flotation process. According to a study, incomplete lithiation of the NMC structure can cause overpotential which in turn reduces the cell capacity significantly [60]. Given that both methods used identical material from the same Nissan LEAF battery, it may suggest that the loss of lithium inventory occurred during the froth flotation process. This can be explained using other studies which suggest that NMC materials tend to undergo delithiation of oxides and formation of LiOH and Li_2CO_3 upon exposure to moisture or humid air [58,60]. The studies also suggest that these changes are partially reversible by electrochemical relithiation of the oxide which explains the gradual increase in the capacity while vanishing overpotential in the 5th cycle curve. However, as these changes are not completely reversible, a lower capacity was still observed for froth flotation samples compared to ultrasonication samples even at the 5th cycle. Ultrasonication samples remained similar capacity over 5 cycles and the nature of the charge-discharge curve was not changed significantly.

Results demonstrate that the ultrasonication-based separation technique developed in this study is effective in separating cathode materials while maintaining the structural, chemical, and electrochemical characteristics of the materials. Thus, the method was proved to be utilized for the next step, relithiation process.

3.2 Heat Treatment Effects

Heat treatment has been known as an important part of cathode regeneration. The purposes of heat treatment are threefold: 1) repairing structural defects of used cathode materials, 2) promoting the crystallization of used cathode materials to form desired phases, and 3) removing impurities (e.g., PVDF binder, carbon black, surface layer) on used cathode materials. This process can be carried out before or after relithiation process. Previous studies indicated that heat treatment processes affect cathode materials in various ways depending on material composition and chemistry. To study the effect of heat treatment on cathode regeneration, we investigated two battery chemistries: LCO and LMO/NMC cases.

3.2.1 IPAD2 Cell: LCO case study

Electrochemistry: To inspect how pre-heat treatment affects LCO regeneration, we used a used iPad cathode material separated by a combination of ultrasonication and centrifuge. The extracted cathode from iPad battery was separated using ultrasonication and the separated material was heated in a furnace at 550 °C for 7 hours. Figure 3.8 represents the comparative charge-discharge curves for before and after heat-treated samples for the 1st and 5th cycle. Apart from the heating process, these materials were processed, cycled, and analyzed under identical conditions. The curves show almost identical 1st cycle performances with slight difference in discharge capacity. For both cases, the discharged capacity was in the range of 120-127 mAh/g. The difference was not significant as sample to sample variation was in the range of 1-10 mAh/g. However, it shows a drastic change after the 5th cycle. The sample without heat treatment showed a gradual decline in the discharge capacity over 5 cycles, reaching around 95-100 mAh/g after the 5th cycle. After that, a stable capacity remained in that range. However, in the case of the heat-treated sample, the

capacity did not change over 5 cycles and the 1st discharge capacity remained after 5 cycles. This result was confirmed by multiple samples. All of the unheated samples created the similar pattern of steady declination while most of the heated samples maintained the higher capacity observed in the 1st cycle. It suggests that pre-heat treatment before relithiation process can be beneficial for LCO.

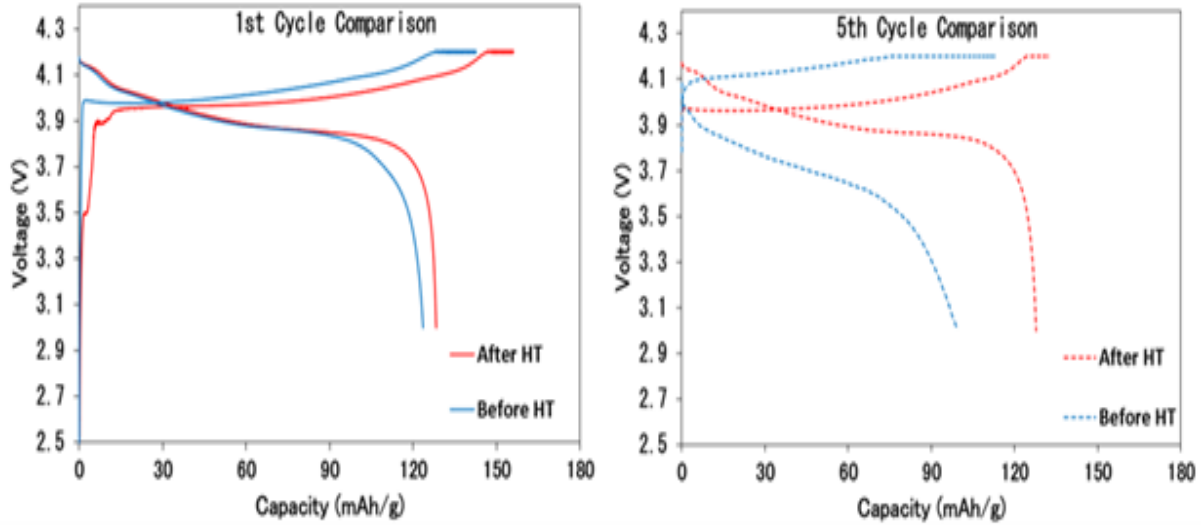


Figure 3.8. The 1st and 5th charge-discharge curves of heat-treated and non-heat-treated iPad cathodes

The stable capacity for heat-treated LCO can be attributed to improved crystallinity and repairing of the damaged structure during heat treatment. Heating LCO at a certain temperature can cause strain removal in LCO particles and repair of the damaged structure. This further results in improved grain sizes and crystallinity which are crucial for cycle stability as it makes the composition and structure more stable. Given the good thermal stability of LCO and iPad batteries being low degraded, no adverse effects of heat treatment were expected.

3.2.2 Nissan LEAF cell: LMO/LMC case study

Electrochemistry: After finding the benefits of heat treatment on LCO regeneration, it was decided to implement the technique on the LEAF batteries with expectations of the same benefit observed in the LCO case, such as increased crystallinity and possible removal of impurities if any. The LEAF battery uses LMO/NMC chemistry and thus it also provided an opportunity to inspect whether heat treatment is beneficial for other cathode chemistries.

The ultrasonically extracted cathode powder of Nissan Leaf battery was heated in a furnace at 500 °C for 6 hours before making the electrodes. For electrode and cell fabrication, similar conditions were used for heat-treated and non-heat-treated samples. The cells were cycled under identical protocols to inspect any alteration in the electrochemical behavior caused by heat treatment. Figure 3.9 represents the initial charge and discharge curves for both before and after heat treatment cells.

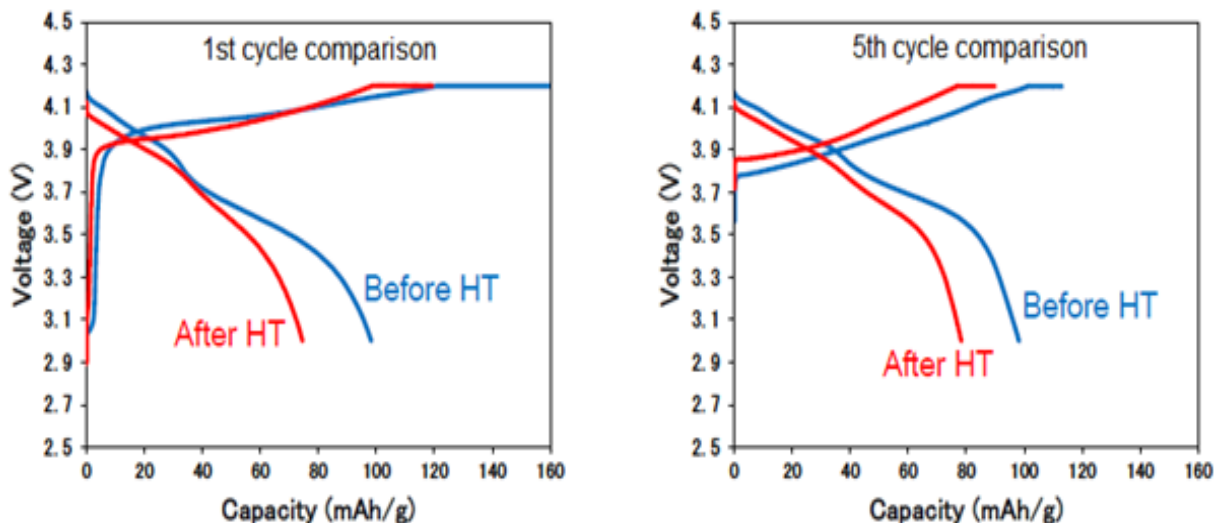


Figure 3.9. The 1st and 5th charge-discharge curves of heat-treated and non-heat-treated LEAF cathodes

As shown in figure 3.9 (left), it was observed that the high resistance and overpotential seen in non-heat-treated cathodes were significantly reduced after heat treatment. This may indicate that heat treatment was effective in improving the degree of crystallinity of the material [60]. However, a significant reduction in capacity was observed. Approximately, the capacity of 75-80 mAh/g was observed for the heat-treated sample, which is approximately

a 20-25% reduction in capacity compared with that of the non-heat-treated sample. This capacity difference almost remained over 5 cycles and no increase in capacity was observed at the 5th cycle. To eliminate possible errors and confirm the repeatability of results, more samples were tested with identical protocols. Figure 3.10 shows the average capacity observed for three samples per each case. The result confirmed that there was an average 20% reduction in capacity at the 5th cycle in the case of the cells with heat-treated cathodes. The reduction in capacity can be an outcome of alteration in the chemical/structural composition of the cathode at higher temperatures. Delithiated cathode materials are susceptible to high temperatures and their decomposition temperatures are lower than pristine cathode materials [61]. Therefore, the formation of undesirable phases or structural changes in the material may affect the reduction in capacity for heat-treated samples. To better understand how LMO/NMC cathode behaves at different temperatures and when decomposition can occur, the effects of high temperatures on LMO/NMC cathode were investigated with XRD analysis.

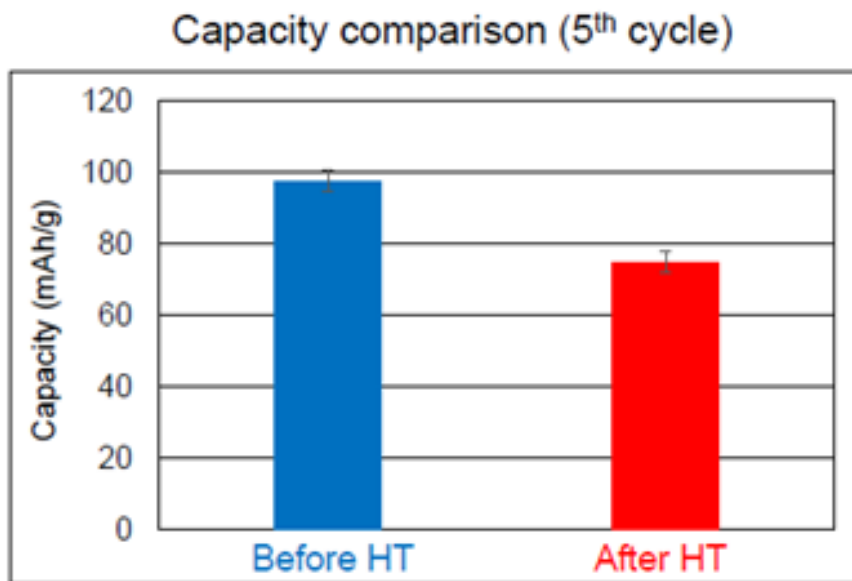


Figure 3.10. Average discharged capacity observed at the 5th cycle in cells before and after heat treatment

XRD characterization: To understand the effects of heat treatment on delithiated or used LMO/NMC cathode, XRD was performed. Literature suggests that a wide range of temperatures can have effects on LMO [61, 62]. Hence, we performed XRD on 4 different samples to cover all the reported temperature range. One sample was unheated to be used as the reference while other samples were heated in a furnace at 300 °C, 500 °C, and 700 °C, respectively. Figure 3.11 shows the XRD plots and comparison between all 4 samples.

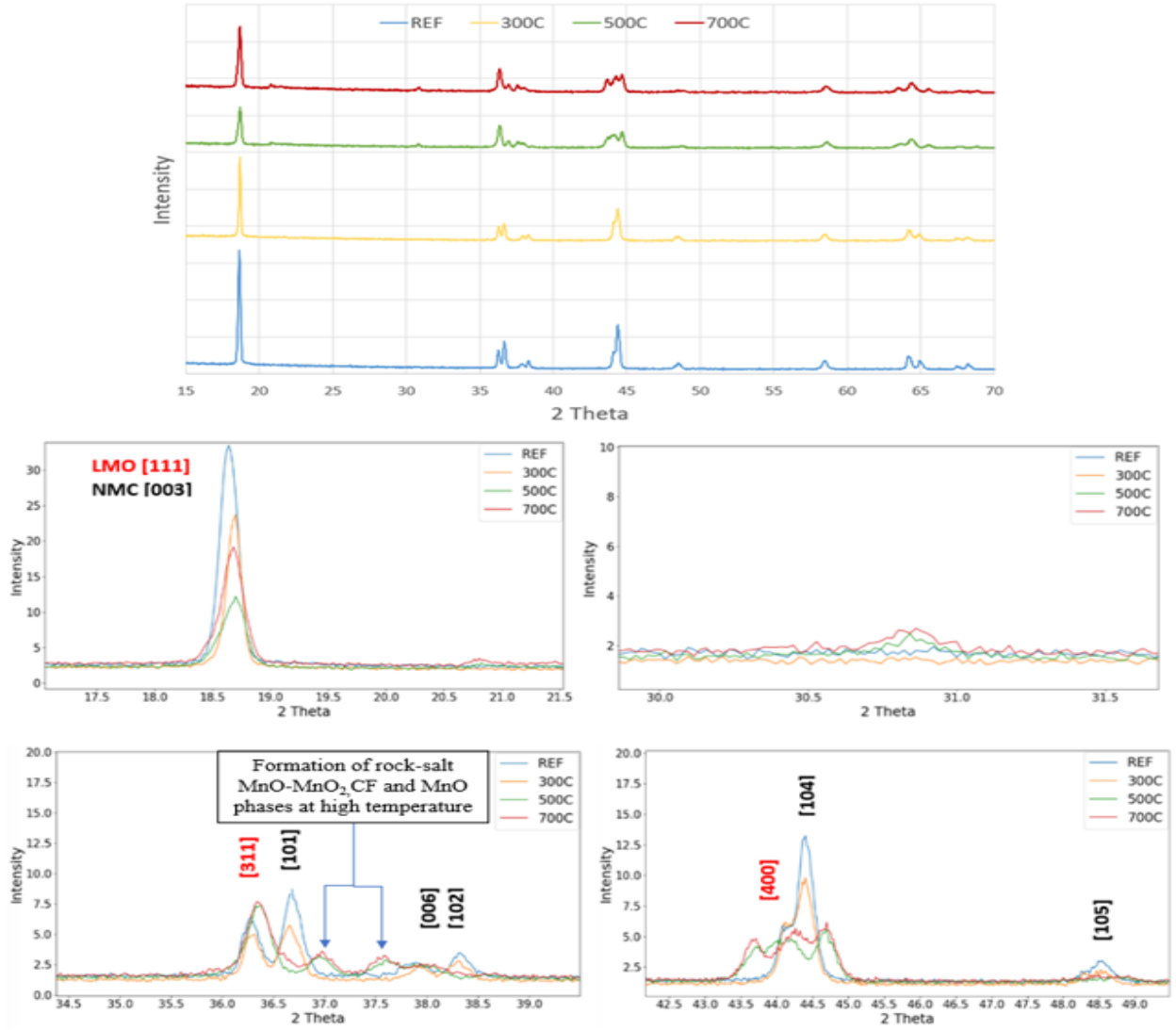


Figure 3.11. The XRD patterns as observed for the reference unheated sample, 300 °C sample, 500 °C sample, and 700 °C sample

There are interesting phenomena observed in the XRD pattern. Firstly, there is a certain decrease in the overall intensity of the curve can be seen in the samples heated at 500 °C and above, as shown in the first graph. The peak representing LMO (111) and NMC (003) between 2 theta angles of 18 and 19 also appears to have slightly shifted to its right. All heat-treated samples (300, 500, 700) show the same peak position. However, as temperature increases, peak broadening is observed with the 500 °C sample showing the most broadening and the lowest intensity. This can be an indication of strain removal which usually occurs in powders after annealing. An increase in the degree of crystallinity leads to strain removal and hence the slight shift in peak position may indicate better crystallinity which is the purpose of heat treatment [61].

At the 2 theta angles between 28-32 degrees, as seen in the 2nd sub-plot, a short new peak appears at temperatures of 500 °C and above samples. Similarly, at the 2 theta angles of 43-45 degrees (the 4th sub-plot), the formation of a new peak is visible in 500 °C and 700 °C samples at 43.5 degrees. In addition, a significant peak broadening can be seen at the peaks representing LMO [400] and NMC [104] in the case of 5000 C and 7000 C samples. The observed phenomena of peak broadening at higher temperatures as well as some shift in peak positions indicate lattice shrinkage as well as differences in position and distribution lithium atom in the spinel crystal structure. Based on the literature, at a higher temperature of above 425 °C, LiMn_2O_4 spinel can be decomposed into three phases of Li_2MnO_3 , MnO-MnO_2 , and Mn_2O_3 which can explain the formation of new peaks at around 37 degrees [61,62]. These compounds further start to transform into the CF-LMO structure at temperatures higher than 525 0 C. This can explain the appearance of a peak around 43.5 degrees in and both 500°C and 700 °C samples.

Furthermore, as seen in the 3rd sub-plot, at the 2 theta angles of 36-39 degrees, some significant changes in XRD patterns are observed. The LMO [311] peak is intensified at heated samples while the subsequent peak representing NMC [101] completely disappears. Besides, the formation of new peaks at 37 and 37.5 degrees occurs. The original peaks seem to be shifted on the right with peak broadening. This can be explained based on a study [62]. It suggests that the decomposition increases with an increase in temperatures between 225 °C to 425 °C and above, and there is the formation of Mn_3O_4 and MnO phases where Mn_3O_4

is dominant. The symmetry of the formed Mn_3O_4 is lowered from cubic to tetragonal due to the cooperative Jahn-Teller distortion of trivalent manganese ions which leads to a rise in Bragg peaks in the XRD pattern. The peak shift around 2 Theta values of 36 and 45 can be associated with an increased Bragg peak of spinel Mn_3O_4 compared with regular cubic spinel structure [62]. These changes are reversible and do not tend to have massive effects on cycling performance. However, upon further increasing the temperature above 425 °C, the material further decomposes to MnO and MnO_2 which forms a rock-salt structure. The formation of those structures is associated with shifts in the peaks as seen in XRD [62].

Similarly, delithiated NMC is unstable at high temperatures. The LMO/NMC cathode material initiates the formation of two types of rock salt phases simultaneously instead of one in case of only LMO being used. The disappearance of NMC [101] is associated with a temperature above 480 °C. At this point, decomposition triggers the formation of MnO rock salt phase as well as there is the formation of another solid solution type rock-salt phase denoted as $(\text{Mn}, \text{Co}, \text{Ni})\text{O}$ [61,62]. These structures forming at higher temperatures can decrease the cycling ability significantly and the effects of heating at these temperatures are irreversible in most cases. It is also observed that delithiated materials tend to see these effects more prominently [62].

Although this increase in crystallinity in early phases of heat treatment is seen, several other structural changes occur throughout the temperature range, most of which resulting in undesired phases. These changes can be associated with some alteration in peak patterns seen in the XRD data. Most of the decomposition phase occurring at comparatively, lower temperatures in the proximity of 224-400 °C tend to be harmless and reversible. However, at temperatures higher than 425 °C, the rock salt structure formations lead to a decrease in capacity which explains the results seen during electrochemical cycling. The decomposition effects are further worsened by higher delithiation and the presence of electrolytic impurities in the extracted cathode material as the thermal stability significantly decreases due to these factors and due to the fact that these changes tend to be irreversible [61]. Based on this observation, it can be concluded that the drawbacks of heat treatment of extracted LEAF powder far outweigh the benefits.

3.3 Relithiation Process Effects

3.3.1 Molar ratio effect

Hydrothermal synthesis can be subjected to a wide range of variations in the conditions and parameters such as temperature, synthesis time, drying temperature, and lithiation agent. Although all these factors are critical in determining the results of the process, some factors have a huge impact compared to others. One of the most important factors is the concentration of lithium salt used. The amount of lithium salt to be added is measured based on the molar ratio for lithium between the active material and the lithium salt. The effects of different molar ratios (AM:LiOH, 1:1 vs. 1:5) on LEAF cathode regeneration are discussed by evaluating the electrochemical performance of the regenerated cathodes in this section. Figure 3.12 shows the cycling performance observed at the 2th cycle for comparison for Nissan LEAF material extracted and further regenerated using 1:1 and 1:5 molar ratio. Compared to the sample regenerated hydrothermally with the 1:1 molar ratio, the sample regenerated with the 1:5 molar ratio shows a higher discharge capacity. The observed discharge capacity of 120 mAh/g is even higher than that of the reference sample (before hydrothermal synthesis). This indicates that a larger amount of lithium is reinserted into the lattice structure of the material via hydrothermal synthesis having the molar ratio of 1:5. Thus, it can be concluded that hydrothermal synthesis with a higher concentration of lithium salt is effective in regenerating spent cathode materials compared to the synthesis with a lower concentration of lithium salt.

It is noted that the sample regenerated with the 1:1 molar ratio shows a slightly lower capacity than that observed for the reference sample. This may indicate that no relithiation occurs in the case of the regeneration with 1:1 molar ratio. In addition, both hydrothermally regenerated cathodes display a higher CV charge capacity, which is an indication of high internal resistance. This means that the usage of different molar ratios for hydrothermal synthesis has no impact on reducing internal resistance.

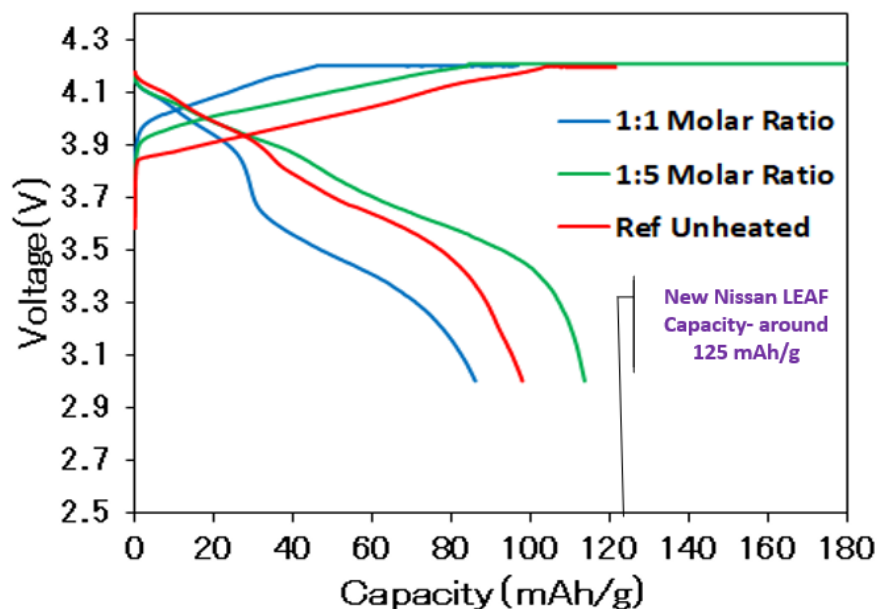


Figure 3.12. The 2nd charge-discharge curves of regenerated samples via hydrothermal synthesis with AM: LiOH ratios 1:1 and 1:5 and reference sample

SEM characterization: To understand structural and morphological changes if any, have occurred during the processes employed, SEM analysis was conducted under different resolutions. Figure 3.13 shows SEM images of hydrothermally regenerated LEAF powder samples. The material structure appears to be intact with no visible cracks in the active material particles, further confirming that neither the ultrasonication-based liberation process nor hydrothermal synthesis reaction has any adverse effects on the structural and morphological properties of the material. Besides, when compared to the SEM images of the reference sample (before hydrothermal synthesis), the hydrothermally regenerated sample does not show any significant morphological changes. Although the success of lithiation cannot be determined based on SEM images only, SEM analysis confirms that no significant changes in structure and morphology occurred during hydrothermal regeneration process.

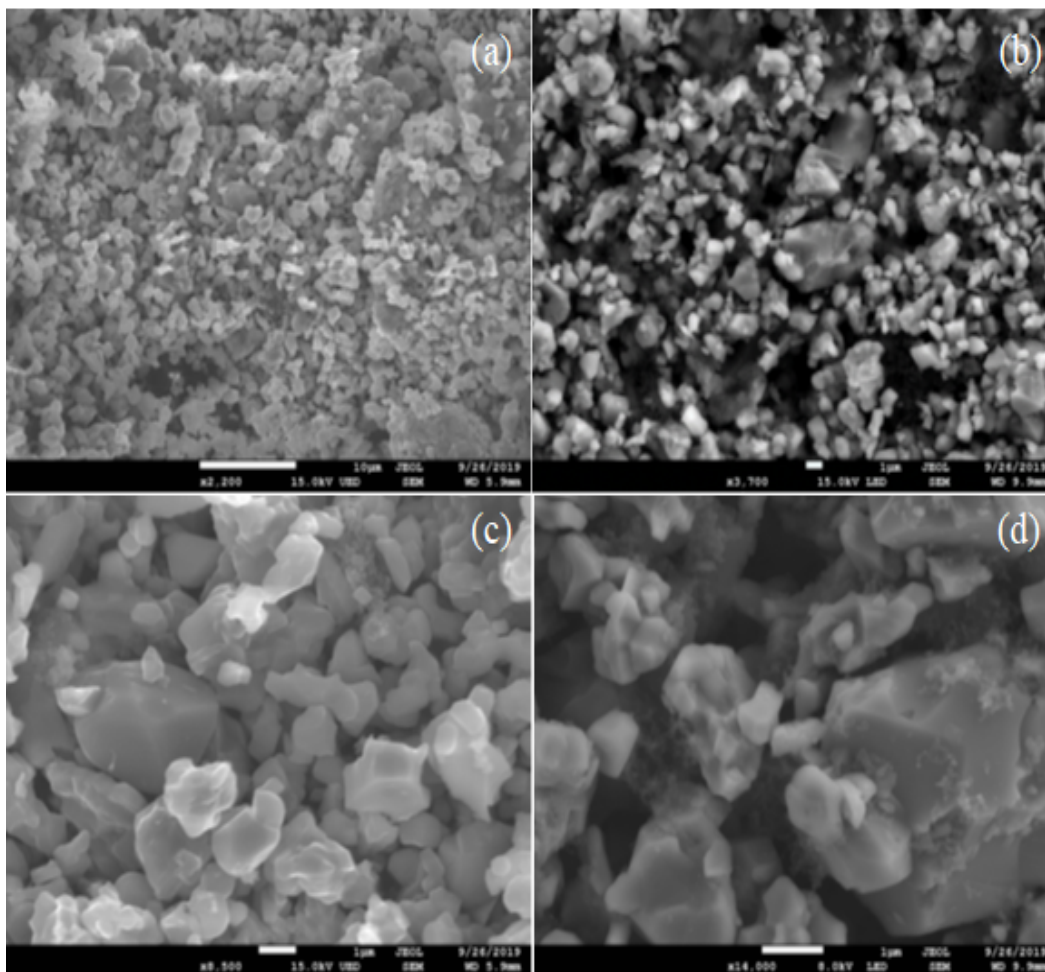


Figure 3.13. SEM images of hydrothermally regenerated cathode powder (a, c) and reference cathode powder (b, d)

3.3.2 Solvent effect (hydrothermal vs. solvothermal)

Based on our observation on the electrochemical performance of cathodes separated by froth flotation, the use of water in hydrothermal process may have detrimental effects on cathode materials. Although cathode regeneration with hydrothermal synthesis with a higher molar ratio 1:5 was successful, the sample still showed a higher CV charge capacity compared to the reference sample. In addition, the sample regenerated hydrothermally with a lower molar ratio 1:1 depletion in discharge capacity compared to the reference sample. It was speculated that exposing delithiated cathode material to a large amount of water during hydrothermal regeneration might be a potential reason. Eliminating water from the process

may have a positive impact on cathode regeneration. Therefore, we investigated whether a solvothermal process, in which Triethylene glycol (TEG) is used as a solvent, can be effective in cathode regeneration. TEG as a solvent can function perfectly as a replacement for water in the hydrothermal synthesis. It is used in industry as a dehydrant due to its hygroscopic quality and its ability to dehumidify substance. It is also a colorless and odorless liquid with high stability. Hence to study the damage to the material due to exposure to moisture and essentially eliminate it, TEG is effective. Conducting this experiment would provide an opportunity to inspect the effects of solvent used in hydrothermal regeneration, which is far less studied previously compared to other parameters of hydrothermal synthesis such as molar ratio and temperature.

The process parameters and equipment were kept identical to that of hydrothermal synthesis and was carried out with a molar ratio of 1:1 at around 180 °C for 22 hours. Fabricated cells from the electrode used the same cycling protocol as what was used for hydrothermal cells. Figure 3.14 shows the comparison of charge-discharge curves for the 5th cycle between reference, hydrothermal, and solvothermal samples. The data of 'Ref' i.e. reference sample indicates the material extracted from Nissan LEAF batteries using ultrasonication which is directly used to make and test coin cell without any lithiation efforts while 'Hydrothermal' and 'Solvothermal' samples indicate the data for the same reference material further regenerated using respective techniques.

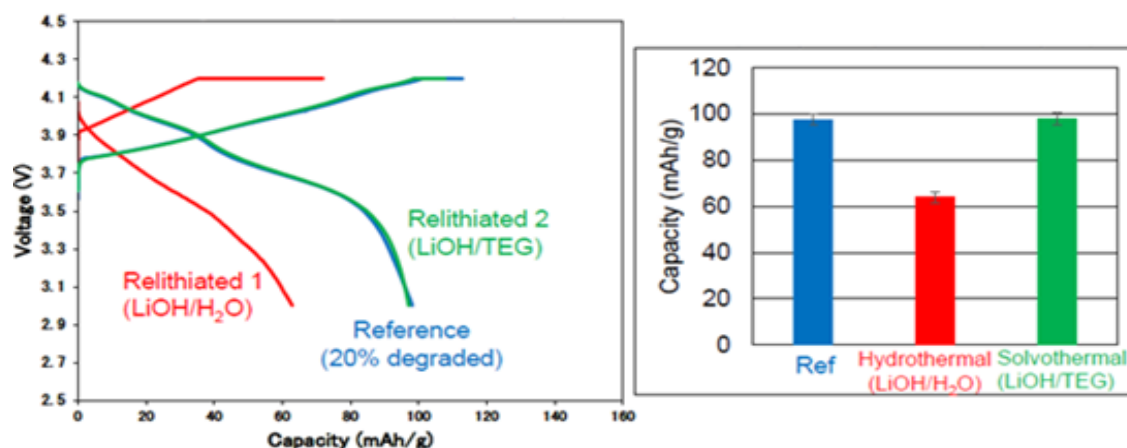


Figure 3.14. The 5th charge and discharge curves of reference, hydrothermal, and solvothermal samples and their capacity comparison

Solvothermal samples showed a significantly better electrochemical performance as compared to hydrothermal processes. In terms of discharge capacity, the solvothermal process improved spent cathode significantly over hydrothermal process showing the average discharge capacity for the 5th cycle across multiple cells ranging around 100 mAh/g compared to that of 80 mAh/g in the case of hydrothermal electrodes. Besides, the sample regenerated with solvothermal process showed a significantly reduced CV portion of the charge, which indicates a lower resistance compared to the sample regenerated with hydrothermal process. Even though the higher molar ratio hydrothermal synthesis (1:5) was able to improve discharge capacity compared to the reference sample, a large CV portion was still observed. Based on this result, we can conclude that solvothermal process shows better results even at the 1:1 molar ratio as compared to hydrothermal synthesis in terms of an increase in discharge capacity and a decrease in internal resistance.

ICP characterization: To confirm whether relithiation occurs during hydrothermal process, ICP analysis was performed. Even though ICP is a trusted technique to determine the composition of materials, several factors including incomplete digestion can alter the results. Different material has a different solubility in the acid used which may lead to incomplete digestion of less soluble materials. Although we used an optimized method for digestion as described in methodology chapter 2, we verified our method by testing materials with known compositions (NMC532). For method verification, we used IUPUI Ref sample (LEAF cathode) which is a combination of NMC and LMO materials extracted from Nissan LEAF batteries using ultrasonication at IUPUI and commercially available standard NMC532 material. Figure 3.13 represents results obtained from reference samples and samples after relithiation process.

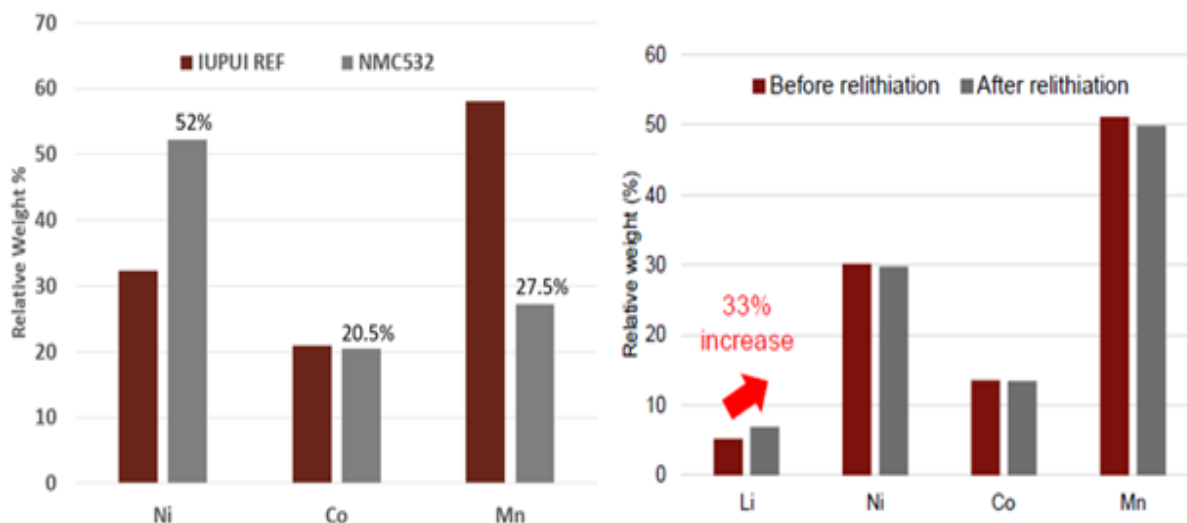


Figure 3.15. Relative weights percentage as determined by ICP for (a) LEAF reference powder and commercial NMC532 powder; (b) separated LEAF powder before and after hydrothermal regeneration

As seen in Figure 3.15a, the NMC532 material showed a relative weight percentage of 52%, 27.5%, and 20.5% for each Ni, Mn, and Co, respectively. This is in the ratio of N:M:C as 5.2:2.75:2.05 which is roughly in 5-3-2 weight proportion which should be present in NMC532. The IUPUI Ref electrode showed a higher weight percentage of Mn and lowered for Ni while maintaining an identical relative weight percentage for Co. As the LEAF electrode is an essentially LMO added to NMC532, an increase in Mn concentration was expected. Additionally, an unchanged percentage in the relative weight of Co signifies the absence of false reading. The results measured by this run were identical to the theoretically expected values. This proves that the digestion technique applied is effective and the results generated by ICP are reliable.

After verifying the ICP technique, ICP tests were further performed on both before and after regeneration samples. The results showed a similar relative weight profile after lithiation as that for before lithiation samples with a slight equivalent decrease in all Ni, Co, and Mn percentages. This decrease was compensated in the increased relative weight percentage of lithium. ICP reported an increase of 33% in the relative weight of lithium after the lithiation process. Based on ICP measurements, it was concluded that the relithiation technique employed is successful in reinserting lithium into spent cathode material.

4. CONCLUSIONS AND FUTURE WORK

4.1 Conclusion

Degraded cathode materials from used LIBs recovered from Nissan LEAF and Apple iPad2 was liberated and separated using ultrasonication combined with a centrifuge. ICP and SEM results demonstrated that the ultrasonication-based liberation/separation technique was successful in maintaining the morphology and chemical composition of both iPad (LCO) and LEAF (LMO/NMC) cathodes. The ultrasonication-based technique is effective in eliminating carbon impurities and binder as seen in SEM and TGA. The electrochemical performance of liberated material was similar to actual cathodes from these used batteries, indicating effective separation. Liberated materials were regenerated using a direct approach technique of hydrothermal regeneration and the effects of heat treatment were studied. Heat treatment of LCO resulted in better crystallinity and improved electrochemical performance and constant discharge capacity throughout cycling, unlike unheated samples. However, heat treatment had adverse effects on delithiated LMO/NMC. A decline in electrochemical performance with around 20% decrease in discharge capacity was seen in LEAF cathode. XRD analysis concluded that the presence of undesirable phases at high temperatures of 500 °C and above. The effects of solvent used in hydrothermal regeneration were studied. The regeneration process did not have any morphological changes as seen in SEM. Using a molar ratio of 1:5 instead of 1:1 between the active material and LiOH resulted in improved cycling performance by up to 25% in terms of specific capacity. The 1:5 molar ratio samples showed a specific discharge capacity of around 120 mAh/g with a cell reaching as high as 127 mAh/g. This observed capacity is similar to that of new batteries made with virgin, non-degraded materials which ranges around 130 mAh/g. However, synthesis in presence of water damaged the delithiated cathode material causing a decline in some aspects of performance. Replacing water with TEG yielded better and more consistent results. ICP proved that reinsertion of lithium occurred during the hydrothermal regeneration process. It is also observed that lower levels of degradation as that seen in iPad cells impose fewer challenges to regeneration as compared to highly degraded, end-of-life cells due to the susceptibility of delithiated samples to used processes and increasing internal resistance. Regenerating used

cells at lower degradation levels indicate better results which can yield long-term benefits. It can also be concluded that the given approach is scalable and can be used on industrial level given the simplicity of involved processes.

4.2 Future Work

The following tasks are recommended for future study.

1. A molar ratio of higher than 1:5 should be employed to analyze its effects.
2. Hydrothermal regeneration using TEG as a solvent with more concentration of lithium salts should be studied.
3. The effects of heat treatment and regeneration using the parameters used here on other commercial LIB cathode chemistries should be inspected on other combinations of materials.
4. Effects of regeneration on long-term cycling of cells should be inspected.

REFERENCES

- [1] E. Kraft, "Growth in the e-mobility market: Climate goals give electric cars and plug-in hybrids a significant boost," *The Roland Berger newsroom*, 2019.
- [2] B. Sandén, "Systems Perspectives on electromobility," Department of Energy and Environment, *Chalmers University of Technology*, 2014.
- [3] The European Commission Staff, "Commission staff working document on the valuation of the Directive 2006/66/EC on batteries and accumulators and waste batteries and accumulators and repealing Directive 91/157/EEC," *The European Commission (EC) Brussels, page 9-11*, 2019.
- [4] M. Winter, T. Placke, "What drives us now and, in the future, Electromobility," *The University of Münster (WWU)*, page 1-24, 2017.
- [5] W. Brian, "Mineral Commodity Summaries MCS 2020," *USGS (U.S. Geological Survey) Publication Warehouse*, 2020.
- [6] B. Huang, Z. Pan, X. Su and L. An, "Recycling of lithium-ion batteries: Recent advances and perspectives," *J. Power Sources*, vol. 399, no. (2018), pp. 274-286, 2018.
- [7] M. Chen, X. Ma, B. Chen, R. Arsenault, P. Karlson, N. Simon and Y. Wang, "Recycling end-of-life electric vehicle lithium-ion batteries,," *Joule*, vol. 3, no. 11, pp. 2622-2646, 2019.
- [8] Y. Wang, N. An, L. Wen, L. Wang, X. Jiang, F. Hou, Y. Yin and J. Liang, "Recent progress on the recycling technology of Li-ion batteries," *Journal of Energy Chemistry*, vol. 55, pp. 391-419, 2020.
- [9] H. Ebrahimzade, G. R. Khayati and M. Schaffie, "Leaching kinetics of valuable metals from waste Li-ion batteries using neural network approach," *J. Mater. Cycles Waste*, pp. 2117-2129, 2018.
- [10] D. Song, X. Wang, E. Zhou, P. Hou and L. Z. F. Guo, "Recovery and heat treatment of the $\text{LiNi}_{1/3}\text{Mn}_{1/3}\text{Co}_{1/3}\text{O}_2$ cathode scrap material for lithium-ion battery," *J. Power Sources*, pp. 348-352, 2013.
- [11] T. Elwert, "Recycling Battery from Electric Vehicles," Springer International Publishing AG, Department of Mineral and Waste processing, *Clausthal University of Technology, Germany*, 2018.
- [12] J. Diekmann, "Ecological Recycling of Lithium-Ion Batteries from Electric Vehicles with focus on Mechanical Processes," *Journal of The Electrochemical Society (ECS)*, p. A6185, 2017.
- [13] L. Yao, Y. Feng and G. Xi, "A new method for the synthesis of $\text{LiNi}_{1/3}\text{Co}_{1/3}\text{Mn}_{1/3}\text{O}_2$ from waste lithium ion batteries," *RSC Advances*, no. 55, pp. 44107-44114., 2015.

- [14] Y. He, X. Yuan, G. Zhang, "A critical review of current technologies for the liberation of electrode materials from foils in the recycling process of spent lithium-ion batteries," *Science of The Total Environment*, vol. 14, pp. 23-82, 2020.
- [15] L. Chen, X. Tang, Y. Zhang, "Process for the recovery of cobalt oxalate from spent lithium-ion batteries," *Hydrometallurgy*, pp. 80-86, 2011.
- [16] J. Chen, Q. Li, J. Song, D. Song, L. Zhang and X. Shi, "Environmentally friendly recycling and effective repairing of cathode powders from spent LiFePO₄ batteries," *Green Chem*, no. 8, pp. 2500-2506, 2016.
- [17] D.S. Kim, J. Sohn, C. Lee, "Simultaneous separation and renovation of lithium cobalt oxide from the cathode of spent lithium-ion rechargeable batteries," *Journal of Power Sources*, vol. 132, pp. 145-149., 2014.
- [18] Q. Dai, "EverBatt: A closed-loop Battery Recycling Cost and Environmental Impacts Model," *Argonne National Laboratory*, United States., 2019.
- [19] I. Buchmann, "BU-705: Battery Recycling as a Business," *Battery University* 705, 2017.
- [20] Fractal Energy Storage Consultants, "The Coronavirus outbreak to impact China's battery storage production". *Power Technology Report*, 2020
- [21] A. Cohan, "Manufacturers are struggling to supply Electric Vehicles with Batteries," *Forbes Magazine*, 2020.
- [22] M. Jacoby, "It's time to get serious about recycling lithium ion batteries," *C&EN*, vol. 97, no. 28, 2019.
- [23] T. Or, "Recycling of mixed cathode lithium-ion batteries for electric vehicles: current status and future outlook," *Carbon Energy Wiley*, 2019.
- [24] L. Gaines, "Lithium-Ion Battery Recycling Processes: Research towards a Sustainable Course," *Argonne National Lab*, United States, 2018.
- [25] H. Hao, Q. Qiao, Z. Liu, F. Zhao, "Impact of recycling on energy consumption and greenhouse gas emission from electric vehicle production: The China 2025 Case," *Resources Conservation and Recycling*, vol. 122, pp. 114-125, 2017.
- [26] A. Boyden, "The environmental impacts of recycling portable lithium-ion batteries," in *23rd CIRP Conference of Life Cycle Engineering*, 2016.
- [27] N. Bensalah, H. Dawood, "Review on Synthesis, Characterizations, and Electrochemical Properties of Cathode Materials for Lithium-Ion Batteries," *Journal of Material Science & Engineering*, vol. 5, no. 4, 2016.
- [28] R. Chen, M. S. Whittingham, "Cathodic behavior of alkali manganese oxides from permanganate," *J. Electrochem. Soc*, vol. 144, pp. L64-L67, 1997.

- [29] M. Broussely, P. Biensan, B. Simon, "Lithium insertion into host materials: the key to success for Li-ion batteries," *Electrochim Acta*, vol. 45, pp. 3-22, 1999.
- [30] M. Thackeray, "Structural Considerations of Layered and Spinel Lithiated Oxides for Lithium Ion Batteries," *Journal of The Electrochemical Society*, vol. 142, no. 8, pp. 2558-2563, 1995.
- [31] G. Amatucci, "The elevated temperature performance of the LiMn₂O₄/C system: failure and solutions," *Electrochimica Acta*, vol. 45(1-2), pp. 255-271, 1999.
- [32] Z. Liu, A. Yu and J.Y. Lee, "Synthesis and characterization of LiNi_{1-x-y}Co_xMn_yO₂ as the cathode materials of secondary lithium batteries," *Journal of Power Sources*, vol. 81-82(0), pp. 416-419, 1999.
- [33] M. Yoshio, "Preparation and properties of LiCo_yMn_xNi_{1-x-y}O₂ as a cathode for lithium ion batteries," *Journal of Power Sources*, vol. 90(2), pp. 176-181, 2000.
- [34] T. Ohzuku and Y. Makimura, "Layered Lithium Insertion Material of LiCo_{1/3}Ni_{1/3}Mn_{1/3}O₂ for Lithium-Ion Batteries," *Chemistry Letters*, vol. 30(7), pp. 642-643, 2001.
- [35] I. Belharouak, "Li(Ni_{1/3}Co_{1/3}Mn_{1/3})O₂ as a suitable cathode for high power applications," *Journal of power sources*, vol. 123, no. 2, pp. 247-252, 2003.
- [36] W.-S. Yoon, "A comparative study on structural changes of LiCo_{1/3}Ni_{1/3}Mn_{1/3}O₂ and LiNi_{0.8}Co_{0.15}Al_{0.05}O₂ during first charge using in situ XRD," *Electrochemistry Communications*, vol. 8(8), pp. 1257-1262, 2006.
- [37] J. Pender, G. Jha, D. Youn, J. Ziegler, "Electrode Degradation in Lithium-Ion Batteries," *ACS Nano*, vol. 14, no. 2, pp. 1243-1295, 2020.
- [38] X. Han, L. Lu, Y. Zheng, X. Feng, "A review on the key issues of the lithium-ion battery degradation among the whole life cycle," *eTransportation*, 2019.
- [39] Chen Liao, "Electrolytes and Additives for Batteries Part I: Introduction and Insights on Cathode Degradation Mechanisms," *eTransportation*, pp. 5, 2020.
- [40] J. Wu, S. Yang, W. Cai, Z. Bi, G. Shang and J. Yao, "Multi-characterization of LiCoO₂ cathode films using advanced AFM-based techniques with high resolution," *Sci. Rep.*, vol. 7, pp. 1-9, 2017.
- [41] J. Vetter, P. Novák, M. R. Wagner, C. Veit, K.-C. Möller, J. O. Besenhard, M. Winter, M. Wohlfahrt-Mehrens, C. Vogler and J. Hammouche, "Ageing mechanisms in lithium-ion batteries," *Power Sources*, vol. 147, pp. 269-281, 2005.
- [42] X. Hao, X. Lin, W. Lu and Bartlett, "Oxygen Vacancies Lead to Loss of Domain Order, Particle Fracture, and Rapid Capacity Fade in Lithium Manganospinel (LiMn₂O₄) Batteries," *ACS Appl. Mater. Interfaces*, vol. 6, pp. 10849-10857, 2014.

- [43] J. Gilbert, J. Bareño, T. Spila, S. Trask, "Cycling Behavior of NCM523/Graphite Lithium-Ion Cells in the 3-4.4 V Range: Diagnostic Studies of Full Cells and Harvested Electrodes," *J Electrochem Soc*, vol. 10.1, 2017.
- [44] H. Wang, J. Whitacre, "Direct Recycling of Aged LiMn₂O₄ Cathode Materials used in Aqueous Lithium-ion Batteries: Processes and Sensitivities," *Energy Technology*, vol. 6, pp. 2429 – 2437, 2018.
- [45] E. Hu, S. Bak, S. Senanayake, X. Yang, "Thermal stability in the blended lithium manganese oxide e Lithium nickel cobalt manganese oxide cathode materials: An in-situ time-resolved X-Ray diffraction and mass spectroscopy study," *Journal of Power Sources*, vol. 277, pp. 193-197, 2015.
- [46] J. Chen, et al. "Environmentally friendly recycling and effective repairing of cathode powders from spent LiFePO₄ batteries." *Green Chemistry*, Vol.18, issue: 8, pp. 2500-2506, 2018.
- [47] M. Ganter, et al., "Cathode refunctionalization as a lithium ion battery recycling alternative." *Journal of Power Sources*, Vol. 256; pp. 274-280, 2018.
- [48] D. Kim, et al., "Simultaneous separation and renovation of lithium cobalt oxide from the cathode of spent lithium ion rechargeable batteries." *Journal of Power Sources*, Vol. 132, pp. 145-149, 2014.
- [49] Y. Shi, et al. "Effective regeneration of LiCoO₂ from spent lithium-ion batteries: a direct approach towards high-performance active particles." *Green Chemistry*, Vol. 20; issue:4, pp. 851-862, 2018.
- [50] H. Wang, and J. F. Whitacre, "Direct Recycling of Aged LiMn₂O₄ Cathode Materials used in Aqueous Lithium-ion Batteries: Processes and Sensitivities." *Energy Technology*, Vol. 6; pp. 2429-2437, 2018.
- [51] L. He, S. Sun, X. Song, J. Yu, "Recovery of cathode materials and Al from spent lithium-ion batteries by ultrasonic cleaning," *Waste management*, vol. 8, no. 35, 2015.
- [52] S. Chen, et al., "Renovation of LiCoO₂ with outstanding cycling stability by thermal treatment with Li₂CO₃ from spent Li-ion batteries." *Journal of Energy Storage*, Vol. 8; pp. 262-273, 2016.
- [53] K. Jalkanen, "Cycle aging of commercial NMC/graphite pouch cells at different temperatures", *Applied Energy*, Vol. 154; pp. 160-172, 2015.
- [54] V. Yurkiv, "Oxygen evolution and phase transformation in LCO cathode: A phase-field modeling study", *Computational Materials Science*, Vol. 140; pp. 299–306, 2017.
- [55] T. Marks, et al., "A Guide to Li-Ion Coin-Cell Electrode Making for Academic Researchers", *Journal of The Electrochemical Society*, Vol. 158; issue 1, 2018.

- [56] V. Murray, et al., “A Guide to Full Coin Cell Making for Academic Researchers.” *Journal of The Electrochemical Society*, Vol.166; pp. A329-A333, 2018.
- [57] K. Zhang, T. Xu, R. Jow, “Study of the charging process of a LiCoO₂-based Li-ion battery’, *Journal of Power Sources*, Vol. 160; page no. 1349–1372, 2006.
- [58] L. He, S. Sun, X. Song, J. Yu, “Recovery of cathode materials and Al from spent lithium-ion batteries by ultrasonic cleaning,” *Waste management*, vol. 8, no. 35, 2015.
- [59] L. Chen, “Process for the recovery of cobalt oxalate from spent lithium-ion batteries,” *Hydrometallurgy*, vol. 108, pp. 80-86, 2011.
- [60] J. Kasnatscheew, U. Rodehorst, B. Streipert, S. Wiemers-Meyer, “Learning from Overpotentials in Lithium-Ion Batteries: A Case Study on the LiNi_{1/3}Co_{1/3}Mn_{1/3}O₂ (NCM) Cathode,” *Journal of The Electrochemical Society*, vol. 163, no. 14, pp. A2943-A2950, 2016.
- [61] H. Barkholtz, Y. Preger, S. Ivanov, J. Langendorf, “Multi-scale thermal stability study of commercial lithium-ion batteries as a function of cathode chemistry and state-of-charge,” *Journal of Power Sources*, vol. 435, 2019.
- [62] H. Wang, J. Whitacre, “Direct Recycling of Aged LiMn₂O₄ Cathode Materials used in Aqueous Lithium-ion Batteries: Processes and Sensitivities,” *Energy Technology*, vol. 6, pp. 2429 – 2437, 2018.
- [63] E. Hu, S. Bak, S. Senanayake, X., Yang, K. Nam, “Thermal stability in the blended lithium manganese oxide e Lithium nickel cobalt manganese oxide cathode materials: An in-situ time-resolved X-Ray diffraction and mass spectroscopy study,” *Journal of Power Sources*, vol. 277, pp. 193-197, 2015.